Biochimica et Biophysica Acta 1848 (2015) 1573–1590

Contents lists available at ScienceDirect

Biochimica et Biophysica Acta

journal homepage: www.elsevier.com/locate/bbamem

Interactions between permeant and blocking anions inside the CFTR chloride channel pore

Paul Linsdell *

Department of Physiology & Biophysics, Dalhousie University, PO Box 15000, Halifax, Nova Scotia B3H 4R2, Canada

ARTICLE INFO

Article history:
Received 13 January 2015
Received in revised form 8 April 2015
Accepted 9 April 2015
Available online 17 April 2015

Keywords:
Chloride channel
Cystic fibrosis transmembrane conductance regulator
Ion binding
Multi-ion pore behavior
Open channel block
Site-directed mutagenesis

ABSTRACT

Binding of cytoplasmic anionic open channel blockers within the cystic fibrosis transmembrane conductance regulator (CFTR) Cl^- channel is antagonized by extracellular Cl^-. In the present work, patch clamp recording was used to investigate the interaction between extracellular Cl^- (and other anions) and cytoplasmic $Pt(NO_2)_4^{2-}$ ions inside the CFTR channel pore. In constitutively open (E1371Q-CFTR) channels, these different anions bind to two separate sites, located in the outer and inner vestibules of the pore respectively, in a mutually antagonistic fashion. A mutation in the inner vestibule (I344K) that greatly increased $Pt(NO_2)_4^{2-}$ binding affinity also greatly strengthened antagonistic Cl^-:blocker interactions as well as the voltage-dependence of block. Quantitative analysis of ion binding affinity suggested that the I344K mutation strengthened interactions not only with intracellular $Pt(NO_2)_4^{2-}$ ions but also with extracellular Cl^-, and that altered blocker Cl^-- and voltage-dependence were due to the introduction of a novel type of antagonistic ion:ion interaction inside the pore that was independent of Cl^- binding in the outer vestibule. It is proposed that this mutation alters the arrangement of anion binding sites inside the pore, allowing both Cl^- and $Pt(NO_2)_4^{2-}$ to bind concurrently within the inner vestibule in a strongly mutually antagonistic fashion. However, the I344K mutation does not increase single channel conductance following disruption of Cl^- binding in the outer vestibule in R334Q channels. Implications for the arrangement of ion binding sites in the pore, and their functional consequences for blocker binding and for rapid Cl^- permeation, are discussed.

1. Introduction

Ion channels are defined by their selectivity, the ability to pass specific ionic species at very high rates while effectively excluding others. This selectivity is thought to result from the selective binding of the transported ion to discrete binding sites within the channel pore [1]. Indeed, specific permeant ion binding sites have been observed in the crystal structures of K^+ [2,3], Na^+ [4,5], Ca^{2+} [6] and Cl^- channels [7–12]. This direct structural evidence for ion binding was in fact foreshadowed by longstanding biophysical evidence that permeating ions must bind to discrete sites within ion channel pores [13–16]. Rapid ion permeation is then thought to occur due to mutual repulsion between ions bound concurrently to adjacent sites [14,15,17,18], a mechanism that requires that ion channels have so-called "multi-ion" pores in which more than one permeant ion can bind [13,19–21]. Interactions between concurrently bound ions result in a number of manifestations of so-called "multi-ion pore behaviour" [13].

Biophysical evidence for multi-ion pore behaviour has been obtained in a number of Cl^- channels [22–26], including the cystic fibrosis transmembrane conductance regulator (CFTR) [27–31], the product of the gene that is mutated in cystic fibrosis [32]. By analogy with cation channel permeation mechanisms [14,15,17], it has been proposed that repulsion between concurrently bound Cl^- ions is necessary for rapid Cl^- ion conduction in CFTR [33,34]. One commonly-observed manifestation of multi-ion pore behaviour in CFTR is an antagonistic interaction between permeant and blocking anions within the pore. The CFTR channel is subject to open-channel block by a broad range of cytoplasmic anions that bind within the relatively wide inner vestibule of the pore [35]. In many cases, block by such cytoplasmic anions has been shown to be weakened by *trans*- (i.e. extracellular) Cl^- ions [28–30,36–41] or other small monovalent anions [30]. This antagonistic interaction between ions coming from opposite sides of the membrane is reminiscent of the classical "knock-off" mechanism, whereby an ion bound to one site destabilizes the binding of another ion to a nearby site [13,21,42]. However, the nature of the interactions between different anions that underlie blocker knock-off by *trans*-Cl^- ions in CFTR — as well as the location and molecular bases of the sites in the pore at which interacting anions bind — are not well understood. One potential complicating factor is that different kinds of interactions between extracellular Cl^- ions and intracellular blockers have been proposed for CFTR. First, it is thought that Cl^- ions entering into the pore from the extracellular solution promote the exit of bound blocker ions back into the cytoplasm, perhaps (although not necessarily) *via* repulsive electrostatic interactions

* Tel.: +1 902 494 2265; fax: +1 902 494 1685.
E-mail address: paul.linsdell@dal.ca.

http://dx.doi.org/10.1016/j.bbamem.2015.04.004
0005-2736/

[28–30,36,43]. Such a mechanism would be closely related to the classical knock-off mechanism described above. It has further been proposed that such in-pore interactions involve extracellular Cl^- binding to the outer mouth of the pore, including an interaction with the positively charged side-chain of pore-lining arginine residue R334 [43]. Secondly, it has also been shown that binding of extracellular Cl^- and other anions to a site outside of the pore destabilizes the binding of intracellular blockers, and this is proposed to reflect a long-range conformational change in the channel protein [44–46]. This second, non-pore-mediated effect is thought to require extracellular anion interaction with another arginine residue, R899, located on the extracellular face of the CFTR protein [45,46]. The existence of these different putative mechanisms of *trans*-ion interactions — and failure effectively to separate them — are likely to have complicated previous investigations of ion–ion interactions taking place inside the CFTR channel pore.

The present work investigates in detail the interaction between extracellular anions and a test intracellular blocking anion that occurs within the CFTR channel pore. Open channel block by intracellular $Pt(NO_2)_4^{2-}$ ions has previously been characterized in some detail [31,44,47] and the location of a single binding site within the inner vestibule relatively well defined [47–50]. Binding of $Pt(NO_2)_4^{2-}$ to this site in the inner vestibule affects both Cl^- permeation through the open channel and also channel opening and closing [47], however the effect on Cl^- movement in open channels can be isolated using gating-defective, constitutively open E1371Q-CFTR channels [47]. By isolating open channel blocking effects in this mutant, it was recently shown that mutations close to the blocker binding site in the inner vestibule that increase or decrease apparent $Pt(NO_2)_4^{2-}$ affinity also increased or decreased the ability of extracellular Cl^- ions to antagonize blocker binding [47], although the reason(s) for this apparent change in Cl^-:blocker interactions were not examined. In the present work the ability to isolate effectively ion:ion interactions that occur inside the pore in constitutively open channels, while at the same time using mutations to increase or decrease the binding affinity of this example test blocker, is used to allow important new insight into the nature and molecular basis of ion binding and ion:ion interactions in the CFTR pore. Antagonistic ion:ion interactions inside the pore appear to involve ion binding to separate sites in the outer and inner vestibules. Mutant channels showing high affinity blocker binding also show a new mechanism of ion:ion interactions that is proposed to reflect repulsion between Cl^- and $Pt(NO_2)_4^{2-}$ ions bound concurrently in the inner vestibule. Implications of these different mechanisms of ion:ion interaction that influence blocker binding for the mechanism of rapid Cl^- conduction in the channel are also explored.

2. Materials and methods

Experiments were carried out on baby hamster kidney cells transiently transfected with CFTR, as described in detail previously [49]. Macroscopic currents were recorded from gating-defective, constitutively-open E1371Q channels [49], whereas single channel recording experiments were carried out in a wild type CFTR background. It has previously been shown that, whereas $Pt(NO_2)_4^{2-}$ has complex effects on Cl^- conduction and gating in wild type, effects on conduction are isolated in E1371Q, and that blocking effects on this channel mutant are indistinguishable from those on wild type channels in the open state [47]. Additional mutations were introduced into these two backgrounds using the QuikChange site-directed mutagenesis system (Agilent Technologies, Santa Clara, CA, USA) and verified by DNA sequencing. The putative location and functional roles of each of the mutated residues have been described previously (Fig. 1). Thus, lysine K95, located in the inner vestibule of the pore, interacts with intracellular blocking anions, Cl^- and other permeant anions [35,51,52]; arginine R334, located in the outer vestibule, interacts with extracellular Cl^- [52]; isoleucine I344 in the inner vestibule close to K95, can host a positive charge (following mutagenesis) that can either substitute for, or be additive with, that of K95 in interacting with intracellular anions [35,52]; and arginine R899, located on an extracellular loop of the protein and exposed to the extracellular solution, interacts with extracellular Cl^- [53] and other anions [46] away from the channel pore.

Macroscopic and single-channel CFTR currents were recorded using patch clamp recordings from inside-out membrane patches, as described in detail recently [47,49]. For all macroscopic and single-channel recordings, intracellular (bath) solutions contained (in millimolar) the following: 150 NaCl, 2 $MgCl_2$, 10 *N*-tris[hydroxymethyl]methyl-2-aminoethanesulfonate (TES), 50 μM MgATP, pH 7.4. This low concentration of ATP was used to support channel activity because higher concentrations may cause voltage-dependent block of channel mutants with strong blocker binding [49,50]. E1371Q channel activity is well maintained in inside-out patches under these conditions, and $Pt(NO_2)_4^{2-}$ block is indistinguishable from that at 1 mM ATP [47]. Extracellular solutions were based on this same solution (without ATP) (in millimolar): 150 NaCl, 2 $MgCl_2$, 10 TES, pH 7.4. Extracellular Cl^- was reduced by equimolar replacement of 75–150 mM NaCl with Na gluconate. For experiments with other extracellular anions, solutions were based on (in millimolar) the following: 150 Na gluconate, 2 $MgCl_2$, 10 TES, pH 7.4, and extracellular Na gluconate was partially or completely substituted by NaBr, NaF, $NaClO_4$, $NaNO_3$, NaSCN, or Na formate. Membrane voltages were corrected for liquid junction potentials calculated using pCLAMP software (Molecular Devices, Sunnyvale, CA, USA). Current traces were filtered at 50–150 Hz using an eight-pole Bessel filter, digitized at 250 Hz–1 kHz, and analysed using pCLAMP software. Measurement of macroscopic and single channel current amplitudes, and construction of leak-subtracted macroscopic current–voltage (*I–V*) relationships were carried out as described in detail recently [47,49]. Different concentrations of test open channel blocker potassium tetranitroplatinate ($K_2Pt(NO_2)_4$) were applied directly to the cytoplasmic face of inside-out patches from stock solutions made up in normal intracellular solution. Blocker concentration–inhibition relationships were fitted by the equation:

$$\text{Fractional unblocked current} = 1/\left(1 + \left(\left[Pt(NO_2)_4^{2-}\right]/{}^{Pt}K_D\right)^{nH}\right) \quad (1)$$

where ${}^{Pt}K_D$ is the apparent blocker dissociation constant and *n*H the slope factor or Hill coefficient. As described previously, under most circumstances *n*H was very close to unity, except for experiments using K95Q/E1371Q mutant channels where it was in the range 0.40–0.65. The relationship between ${}^{Pt}K_D$ and membrane potential (*V*) was fitted by the equation:

$${}^{Pt}K_D(V) = {}^{Pt}K_D(0)\exp(-z\delta VF/RT) \quad (2)$$

where zδ is the measured effective valence of the blocking ion (actual valence (z) multiplied by the fraction of the transmembrane electric field apparently experienced during the blocking reaction (δ)). Because this parameter is influenced by a number of factors, and for consistency with earlier studies using $Pt(NO_2)_4^{2-}$ [31,44,45,47,48], zδ is not ascribed any particular physical meaning. *F*, *R* and *T* have their usual thermodynamic meanings. In some cases, because block was so weak at depolarized voltages, data obtained at these voltages was excluded from the fitting procedure.

Competition between intracellular $Pt(NO_2)_4^{2-}$ ions and extracellular Cl^- and other anions was analysed based on a model described by Spassova and Lu [54] for tetraethylammonium (TEA) block of inward rectifier K^+ channels, in which blocking and permeant ions bind to separate sites in the pore in a mutually competitive fashion. This model assumes that permeant and blocking ions coming from different sides of the membrane bind to separate sites; as shown in the Results section, this seems likely for the current work, since mutations in the inner vestibule of the pore alter affinity for intracellular $Pt(NO_2)_4^{2-}$ ions, and a mutation in the outer vestibule disrupts binding of extracellular Cl^- ions. The model also assumes a saturating concentration of intracellular permeant ions. The overall dissociation constant for the channel for Cl^- ions, based on single channel conductance measurements, is ~40 mM [55] and the highest affinity Cl^- binding site in the pore is likely associated with K95 in the inner vestibule [51]. All experiments were carried out at a constant high intracellular [Cl^-] of 154 mM. The observed

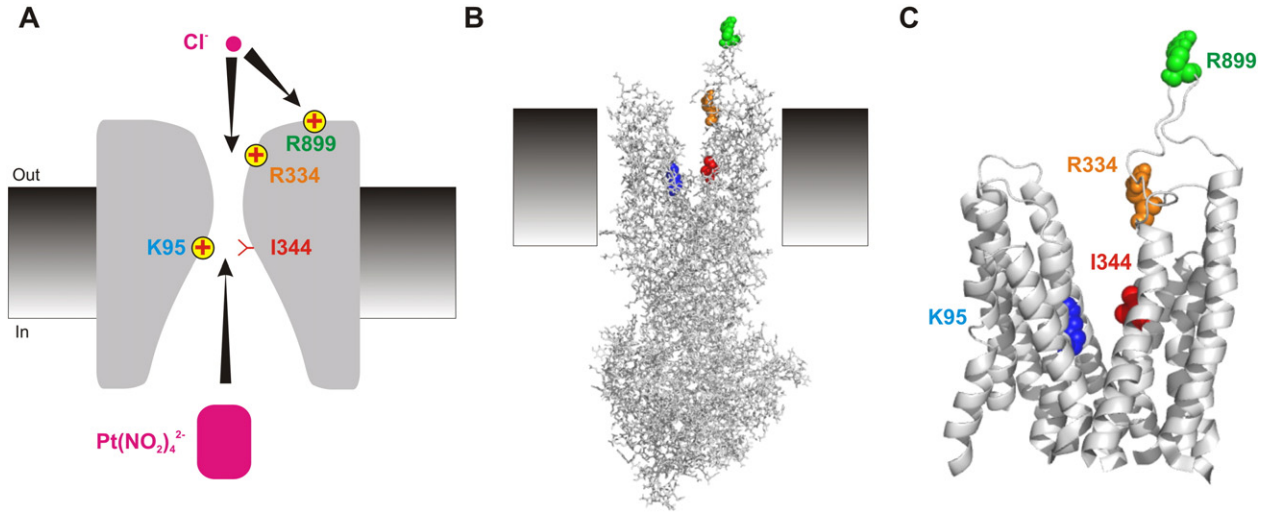

Fig. 1. Proposed location of amino acid residues mutated in the current study. (A) Cartoon model of CFTR pore architecture [52]. Cytoplasmic $Pt(NO_2)_4^{2-}$ ions bind in the wide inner vestibule of the pore, close to K95 and I344 [47,50]. External Cl^- ions are proposed to interact with two independent sites, one inside the pore including R334 [43], and one outside the pore including R899 [53]. For simplicity, a single pathway is shown for $Pt(NO_2)_4^{2-}$ ions to access the pore from the cytoplasm, consistent with longstanding biophysical [52] and pharmacological [35] evidence for a single channel pore, although a recent molecular dynamics study [64] has proposed a more complex access pathway from the cytoplasm to the central pore region. (B, C) Location of these same amino acid residues in a recent atomic homology model of CFTR, illustrated either in the whole protein (B) or in detail of the twelve transmembrane segments (C). In each panel, amino acid residues are shown in the same colour scheme (K95 — blue; R334 — orange; I344 — red; R899 — green). Homology models are based on coordinates provided by Mornon et al. [64] and visualized using PyMol (Schrödinger, LLC, Portland, OR, USA).

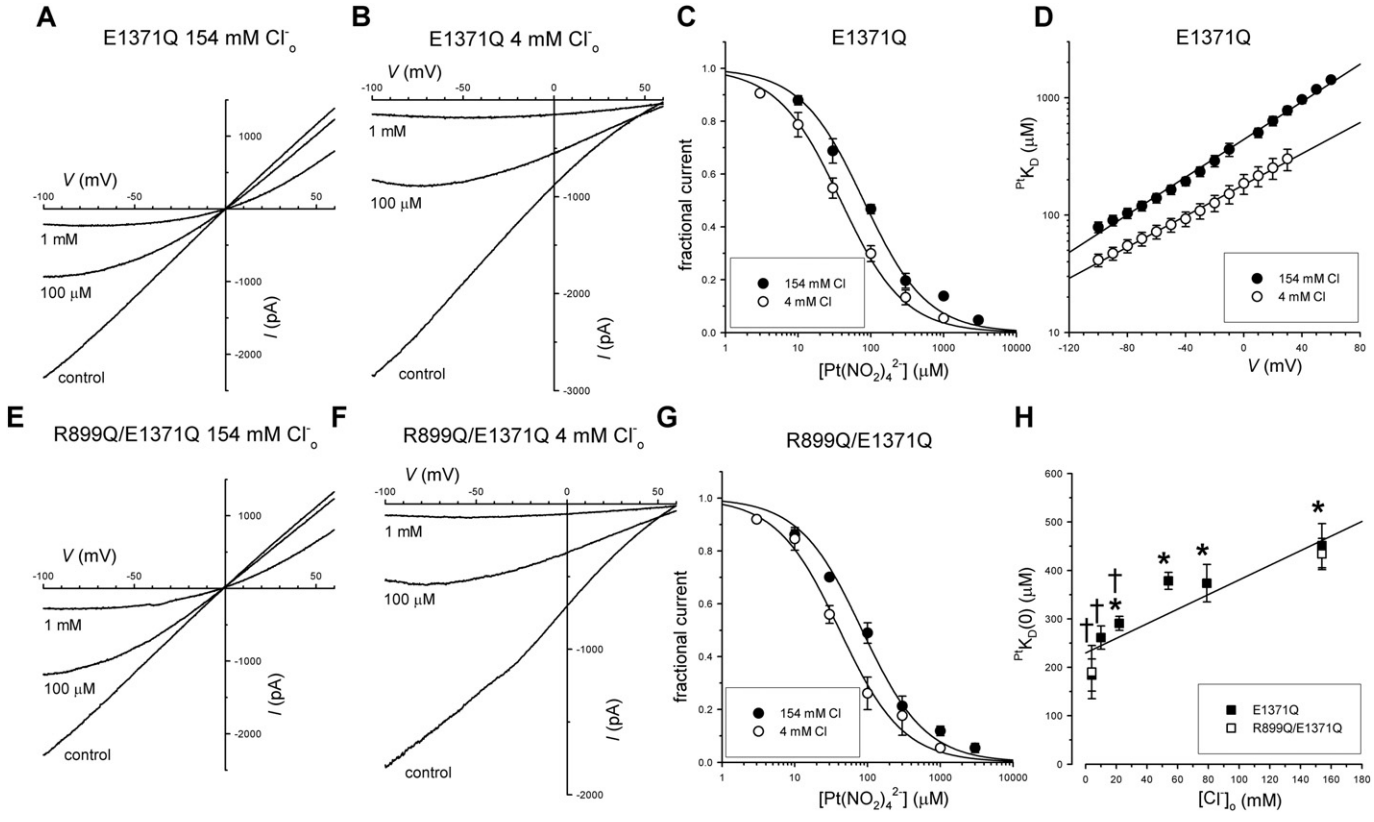

Fig. 2. Block by intracellular $Pt(NO_2)_4^{2-}$ is dependent on extracellular $[Cl^-]$. (A, B, E, F) Example macroscopic *I–V* relationships for E1371Q (A, B) or R899Q/E1371Q (E, F) under high (154 mM; A, E) or low (4 mM; B, F) extracellular $[Cl^-]$ conditions. In each case currents were recorded before (control) and after the addition of 100 μM and 1 mM $Pt(NO_2)_4^{2-}$ to the intracellular solution. (C, G) Mean fraction of control current remaining after addition of different concentrations of $Pt(NO_2)_4^{2-}$ at a membrane potential of −100 mV for E1371Q (C) and R899Q/E1371Q (G) under high (filled circles) and low (open circles) extracellular $[Cl^-]$ conditions. Data have been fitted using Eq. (1) as described in the Materials and methods. (D) Mean $^{Pt}K_D$ values obtained from such fits at different membrane potentials for E1371Q; results for R899Q/E1371Q were indistinguishable (not shown). Data have been fitted using Eq. (2) as described in the Materials and methods. (H) Mean values of $^{Pt}K_D$ at 0 mV membrane potential obtained from fits of $^{Pt}K_D$–*V* relationships such as those shown in D for E1371Q (filled squares) and R899Q/E1371Q (open squares) at different extracellular $[Cl^-]$. Asterisks indicate a significant difference from 4 mM Cl^-_o and daggers indicate a significant difference from 154 mM Cl^-_o ($P < 0.05$). There was no significant difference between E1371Q and R899Q/E1371Q ($P > 0.85$). Mean of data from five to nine patches.

dissociation constant for block by intracellular $Pt(NO_2)_4^{2-}$ ions ($^{Pt}K_D$) at different extracellular $[Cl^-]$ ($[Cl^-]_o$) derives from both the dissociation constant for the internal binding site when the external binding site is occupied by Cl^- ($^{Pt}K_{occ}$) and that when the external binding site is vacant ($^{Pt}K_{vac}$) according to:

$$^{Pt}K_D = {}^{Pt}K_{occ}[Cl^-]_o + {}^{Pt}K_{vac}. \quad (3)$$

This model predicts a linear relationship between $^{Pt}K_D$ and $[Cl^-]_o$, which was reasonably well observed in the present study at different membrane potentials for E1371Q (Figs. 2H, 8A) and pore-mutant CFTR channels (Figs. 4E, J, 6D, H, 8B, C, 10A, B), as well as when extracellular Cl^- was replaced by other anions (Figs. 3D, 7E, F, 11A, E). Straight-line fits to the relationship between $^{Pt}K_D$ and $[Cl^-]_o$ were then used to obtain estimates of $^{Pt}K_{vac}$ (y-axis intercept) and $^{Pt}K_{occ}$ (slope), as well as the dissociation constant for Cl^- binding to the external binding site (^{Cl}K) (intercept/slope).

Experiments were carried out at room temperature, 21–24 °C. Values are presented as mean ± SEM. For graphical presentation of mean values, error bars represent SEM, and where no error bars are shown SEM is smaller than the size of the symbol. Tests of significance were carried out using Student's two-tailed *t*-test, with $P < 0.05$ being considered statistically significant. All chemicals were from Sigma-Aldrich (Oakville, ON, Canada) except for $K_2Pt(NO_2)_4$ (Strem Chemicals, Newburyport, MA, USA) and protein kinase A catalytic subunit (Promega, Madison, WI, USA).

3. Results

3.1. Effect of extracellular anions on block by intracellular $Pt(NO_2)_4^{2-}$

Block of Cl^- movement through open CFTR channels by intracellular $Pt(NO_2)_4^{2-}$ ions is antagonized by extracellular Cl^- ions [31,45,47]. This effect is illustrated for constitutively open E1371Q channels in Fig. 2: $Pt(NO_2)_4^{2-}$ block is strengthened as extracellular Cl^- is replaced by impermeant gluconate anions (Fig. 2C, D), resulting in a monotonic increase in the measured K_D (at 0 mV membrane potential) as extracellular $[Cl^-]$ is increased (Fig. 2H). Identical results were obtained in R899Q/E1371Q channels (Fig. 2; Table 1), both at high and low $[Cl^-]_o$ conditions, indicating that extracellular Cl^- interactions with this externally-located arginine residue (Fig. 1) do not contribute to these antagonistic effects. This confirms that use of the E1371Q background effectively isolates Cl^-:$Pt(NO_2)_4^{2-}$ interactions that occur within the channel pore from those that may involve Cl^- interactions with a non-pore extracellular site.

Other anions may substitute for extracellular Cl^- in antagonizing the binding of intracellular blocking ions inside the pore [30]. Fig. 3A, B illustrates the blocking effects of $Pt(NO_2)_4^{2-}$ when extracellular Cl^- is

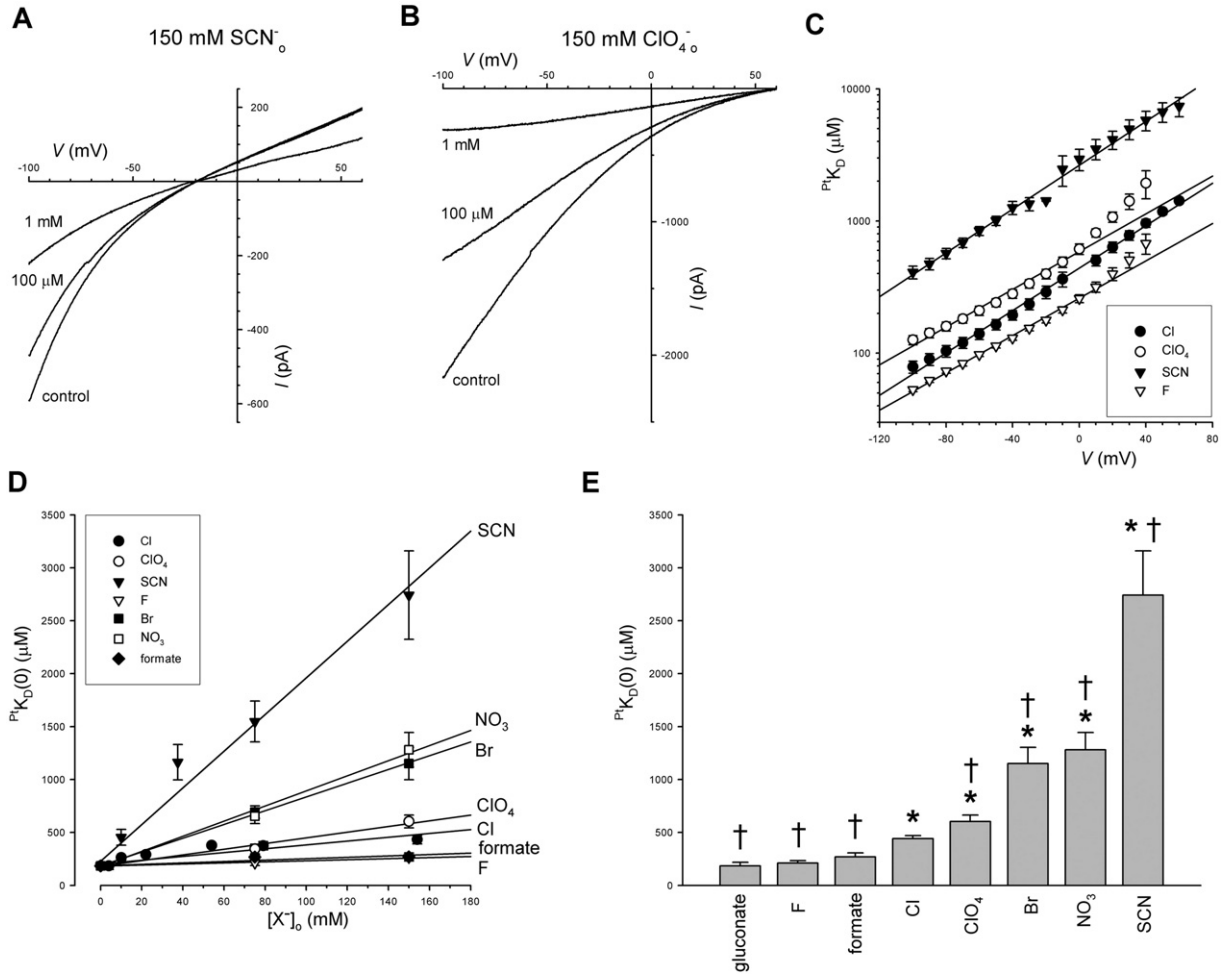

Fig. 3. Effect of other extracellular anions on block by intracellular $Pt(NO_2)_4^{2-}$. (A, B) Example macroscopic *I–V* relationships for E1371Q when the extracellular solution contained 150 mM SCN^- (A) or 150 mM ClO_4^- (B). Currents were recorded before (control) and after the addition of 100 µM and 1 mM $Pt(NO_2)_4^{2-}$ to the intracellular solution. (C) Mean $^{Pt}K_D$ values estimated at different membrane potentials as described in Fig. 2. (D) Mean values of $^{Pt}K_D$ at 0 mV membrane potential under different extracellular anion conditions. (E) Mean values of $^{Pt}K_D$ at 0 mV when the extracellular solution contained 150 mM of the different anions indicated. Asterisks indicate a significant difference from gluconate and daggers indicate a significant difference from Cl^- ($P < 0.0001$). Mean of data from three to nine patches.

Table 1
Observed blocker affinity and voltage dependence in different channel constructs. Mean values of $^{Pt}K_D$ (at 0 mV membrane potential) and zδ were obtained under both low (4 mM) and high (154 mM) $[Cl^-]_o$ conditions as described in Figs. 2, 4 and 6. Asterisks indicate a significant difference from E1371Q (*$P < 0.05$; **$P < 0.001$). Mean of data from the number of patches indicated in parentheses in each case.

	$^{Pt}K_D(0)$ (4 mM Cl^-) (μM)	zδ (4 mM Cl^-)	$^{Pt}K_D(0)$ (154 mM Cl^-) (μM)	zδ (154 mM Cl^-)
E1371Q	183.7 ± 33.2 (9)	−0.397 ± 0.030 (9)	441.0 ± 28.6 (7)	−0.503 ± 0.026 (7)
R899Q/E1371Q	189.9 ± 55.0 (6)	−0.362 ± 0.063 (6)	434.0 ± 32.2 (7)	−0.458 ± 0.048 (7)
K95Q/E1371Q	1110 ± 172 (6)**	−0.244 ± 0.022 (6)*	1422 ± 218 (6)**	−0.193 ± 0.041 (6)**
I344K/E1371Q	6.92 ± 1.48 (6)**	−1.589 ± 0.125 (6)**	164.7 ± 27.5 (7)**	−1.604 ± 0.080 (7)**
R334Q/E1371Q	1081 ± 220 (4)**	−0.637 ± 0.106 (4)*	1112 ± 144 (4)**	−0.621 ± 0.051 (4)*
R334Q/I344K/E1371Q	39.24 ± 7.94 (4)*	−1.093 ± 0.037 (4)**	258.3 ± 30.7 (5)*	−1.075 ± 0.033 (5)**

replaced by SCN^- (which is highly permeant in CFTR [56]) or ClO_4^- (which is sparingly permeant [57]). As with Cl^-, other anions weakened the blocking effects of $Pt(NO_2)_4^{2-}$ (Fig. 3C) in a concentration-dependent fashion, leading to an apparently linear relationship between measured K_D and anion concentration (Fig. 3D). The relative potency of different anions in increasing $^{Pt}K_D$ was $SCN^- > NO_3^- \geq Br^- > ClO_4^- > Cl^- >$ formate ~ F^- (Fig. 3E): formate and F^- anions, in spite of being measurably permeant in CFTR [57], did not significantly increase $^{Pt}K_D$ relative to that measured with impermeant gluconate anions in the extracellular solution.

3.2. Effect of mutations affecting the putative $Pt(NO_2)_4^{2-}$ binding site in the pore

Intracellular $Pt(NO_2)_4^{2-}$ binds within the inner vestibule of the pore, and mutations that alter the number of positive charges in this region decrease or increase the affinity of open channel block [52]. This is illustrated in Fig. 4, under different extracellular $[Cl^-]$ conditions. Thus, K95Q/E1371Q is associated with weakened $Pt(NO_2)_4^{2-}$ block (Fig. 4A–E), and I344K/E1371Q with greatly strengthened block (Fig. 4F–J). These mutations also altered the $[Cl^-]_o$-dependence of block. Thus $^{Pt}K_D$ was only very weakly $[Cl^-]_o$-sensitive in K95Q/E1371Q (Fig. 4E), but very strongly $[Cl^-]_o$-dependent in I344K/E1371Q (Fig. 4J). The affinity, voltage dependence, and $[Cl^-]_o$-dependence of block in E1371Q, K95Q/E1371Q and I344K/E1371Q are compared directly in Fig. 5 and Table 1. These results suggest that the number of positive charges in this part of the pore inner vestibule are correlated not only with the affinity of $Pt(NO_2)_4^{2-}$ block [47] but also with the $[Cl^-]_o$-dependence of block and the voltage-dependence of block: stronger block is both more $[Cl^-]_o$-sensitive (Fig. 5A) and more voltage-dependent (Fig. 5B).

3.3. Effect of mutations on interactions with extracellular anions

Previously it was suggested that a positively charged amino acid side chain close to the extracellular mouth of the pore (at R334; Fig. 1) was required for interactions with extracellular anions [43]. Consistent with this model, neutralization of this charge in the R334Q/E1371Q mutant abolished the relationship between intracellular $Pt(NO_2)_4^{2-}$ block and extracellular $[Cl^-]$ (Fig. 6A–D). Block under low $[Cl^-]$ conditions was weakened by the R334Q mutation (Table 1; also compare results for R334Q/E1371Q in Fig. 6C with E1371Q in Fig. 2D), resulting in a significant increase in $^{Pt}K_D$ at all voltages ($P < 0.002$). This is consistent with earlier findings that mutations at R334 impact the affinity of intracellular blocker binding [43,48]. The R334Q mutation also appeared to increase the voltage-dependence of block (Table 1), although the reasons for this effect are not clear.

Since the R334Q and I344K mutations in different parts of the pore (Fig. 1) had opposite effects on the $[Cl^-]_o$-sensitivity of $Pt(NO_2)_4^{2-}$ block — which was practically abolished in R334Q/E1371Q (Fig. 6) but greatly increased in I344K/E1371Q (Figs. 4, 5) — these mutations were combined to generate a R334Q/I344K/E1371Q mutant. Not only did R334Q/I344K/E1371Q channels exhibit strong $Pt(NO_2)_4^{2-}$ block (Table 1), but block was also strongly dependent on extracellular $[Cl^-]$ (Fig. 6E–H). This confirms that the I344K mutation not only strengthens interactions with intracellular $Pt(NO_2)_4^{2-}$ ions but also with extracellular Cl^- ions. Furthermore, this effect on interactions with extracellular Cl^- appears independent of the presence of a positively charged side chain at position 334: whereas the R334Q mutation abolishes Cl^--dependence of block in E1371Q channels (Fig. 6D), it does not in I344K-bearing E1371Q channels (Fig. 6H). Thus, interactions with external Cl^- that are lost in R334Q/E1371Q channels are at least partially restored by the I344K mutation.

To examine if the I344K mutation also resulted in altered interactions with other extracellular anions — and if this effect was also independent of R334 – $Pt(NO_2)_4^{2-}$ block was also investigated with other extracellular anions, both in I344K/E1371Q and in R334Q/I344K/E1371Q channels (Fig. 7). In both these channel mutants $Pt(NO_2)_4^{2-}$ block was also weakened by other extracellular anions (Fig. 7C–H), with a similar overall apparent anion selectivity to that observed for E1371Q (Fig. 3E). Nevertheless, some specific differences were noted. First, SCN^- had a very strong negative effect on $Pt(NO_2)_4^{2-}$ block in I344K/E1371Q, increasing $^{Pt}K_D(0)$ >600-fold relative to that with gluconate and >25-fold relative to that with Cl^- (Fig. 7C, E, G). Secondly, formate was able to significantly increase $^{Pt}K_D(0)$ relative to gluconate in both I344K/E1371Q (Fig. 7G) and in R334Q/I344K/E1371Q (Fig. 7H), unlike in E1371Q where formate had no significant effect (Fig. 3D, E).

3.4. A quantitative model of anion binding

In constitutively open E1371Q channels, extracellular Cl^- (Fig. 2) and other monovalent anions (Fig. 3) weaken the blocking effects of $Pt(NO_2)_4^{2-}$, suggesting that these anions compete for binding inside the channel pore. Since the binding site for impermeant $Pt(NO_2)_4^{2-}$ ions is thought to be within the inner vestibule, close to K95 and I344 (Fig. 1), and Cl^- binding that antagonizes $Pt(NO_2)_4^{2-}$ binding appears dependent on Cl^- interaction with R334 in the outer vestibule (Fig. 1; Fig. 6A–D), the simplest explanation of this competition is that binding of Cl^- and $Pt(NO_2)_4^{2-}$ to different sites is mutually antagonistic, as proposed earlier for blocker binding in CFTR [28,30] and other ion channels [54,58–61]. Competition between intracellular $Pt(NO_2)_4^{2-}$ and extracellular Cl^- (or other anions) is consistent with the approximately linear relationship between $^{Pt}K_D$ and extracellular anion concentration (Figs. 2H, 3D). As described previously for intracellular TEA block of inward rectifier K^+ channels [54], analysis of the relationship between $^{Pt}K_D$ and extracellular Cl^- allows quantitative description of the affinity of the channel for intracellular $Pt(NO_2)_4^{2-}$ when the external Cl^- binding site is vacant ($^{Pt}K_{vac}$) and when it is occupied by Cl^- ($^{Pt}K_{occ}$), as well as the channel affinity for external Cl^- ions (^{Cl}K) (see Materials and methods for details). Fits to mean data for E1371Q using Eq. (3) (Fig. 8A) suggest, at 0 mV membrane potential, a $^{Pt}K_{vac}$ of 245 μM (Fig. 8D), $^{Pt}K_{occ}$ of 1440 μM (Fig. 8E), and ^{Cl}K 179 mM (Fig. 8F), with voltage dependencies of these parameters suggesting $^{Pt}z\delta_{vac}$ of −0.39 (Fig. 8D), $^{Pt}z\delta_{occ}$ −0.63 (Fig. 8E), and $^{Cl}z\delta$ +0.22 (Fig. 8F). These values (summarized in Table 2) suggest that internal $Pt(NO_2)_4^{2-}$ binds to the channel much less strongly when the external Cl^- binding site is occupied ($^{Pt}K_{vac} < {}^{Pt}K_{occ}$) (Fig. 9A); that both $Pt(NO_2)_4^{2-}$ and Cl^- cross only a relatively small part of the transmembrane electric field to reach their binding sites in the inner and outer vestibules respectively; and that

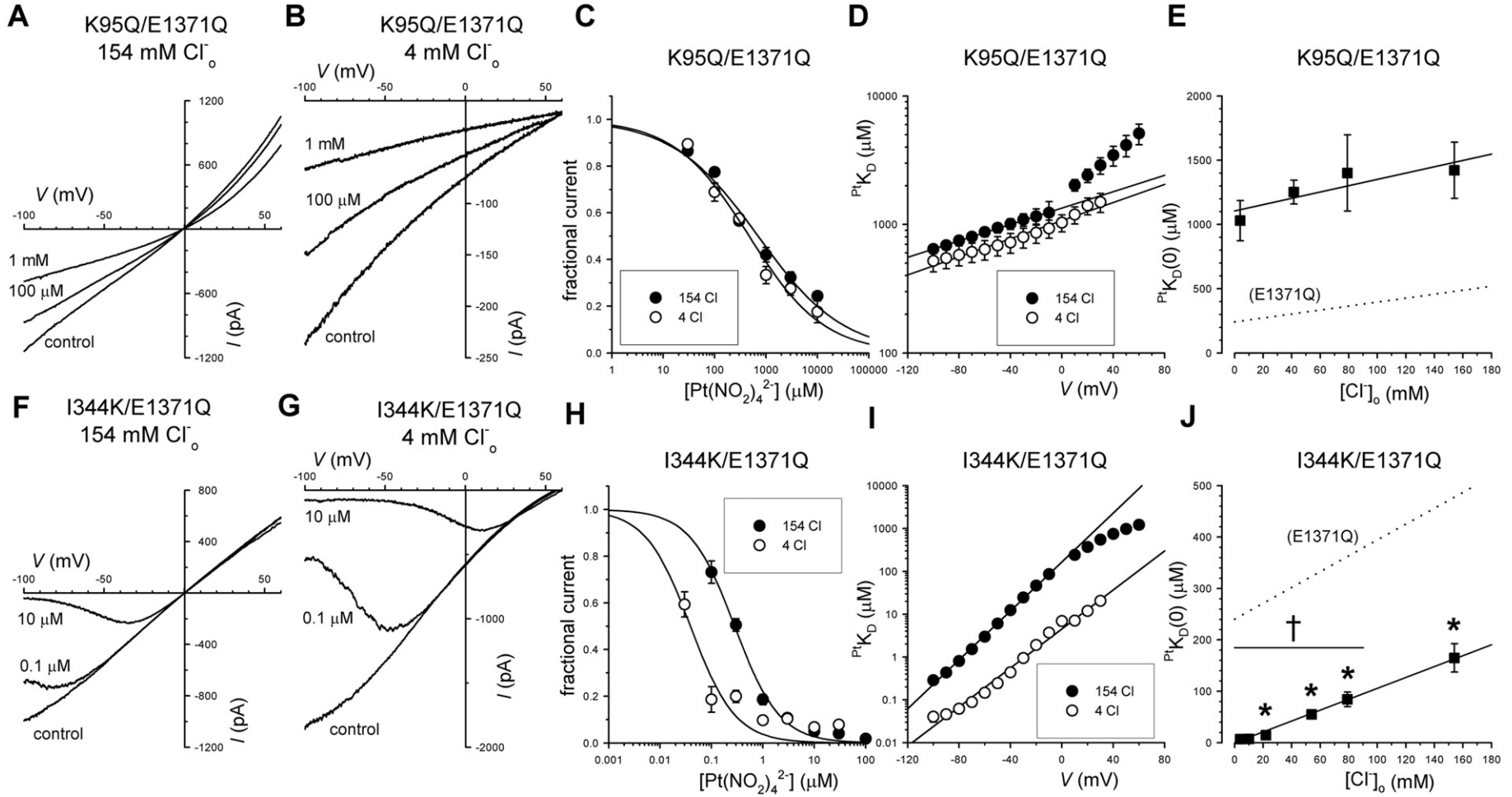

Fig. 4. Effect of mutations that weaken or strengthen intracellular $Pt(NO_2)_4^{2-}$ block. (A, B, F, G) Example macroscopic *I–V* relationships for K95Q/E1371Q (A, B) or I344K/E1371Q (F, G) under high (154 mM; A, F) or low (4 mM; B, G) extracellular [Cl^-] conditions. In each case currents were recorded before (control) and after the addition of $Pt(NO_2)_4^{2-}$ (at the concentrations indicated) to the intracellular solution. (C, H) Mean fraction of control current remaining after addition of different concentrations of $Pt(NO_2)_4^{2-}$ at a membrane potential of −100 mV under high (filled circles) and low (open circles) extracellular [Cl^-] conditions. Data have been fitted using Eq. (1) as described in the Materials and methods. (D, I) Mean $^{Pt}K_D$ values obtained from such fits at different membrane potentials. Data fitted using Eq. (2) as described in the Materials and methods. (E, J) Mean values of $^{Pt}K_D$ at 0 mV membrane potential obtained from fits of $^{Pt}K_D$–*V* relationships at different extracellular [Cl^-]. Asterisks indicate a significant difference from 4 mM Cl^-_o and dagger indicates a significant difference from 154 mM Cl^-_o ($P < 0.05$). There was no significant difference in these parameters for K95Q/E1371Q (E) ($P > 0.05$). Dotted line indicates the fit to data for E1371Q (see Fig. 2H). Mean of data from three to seven patches.

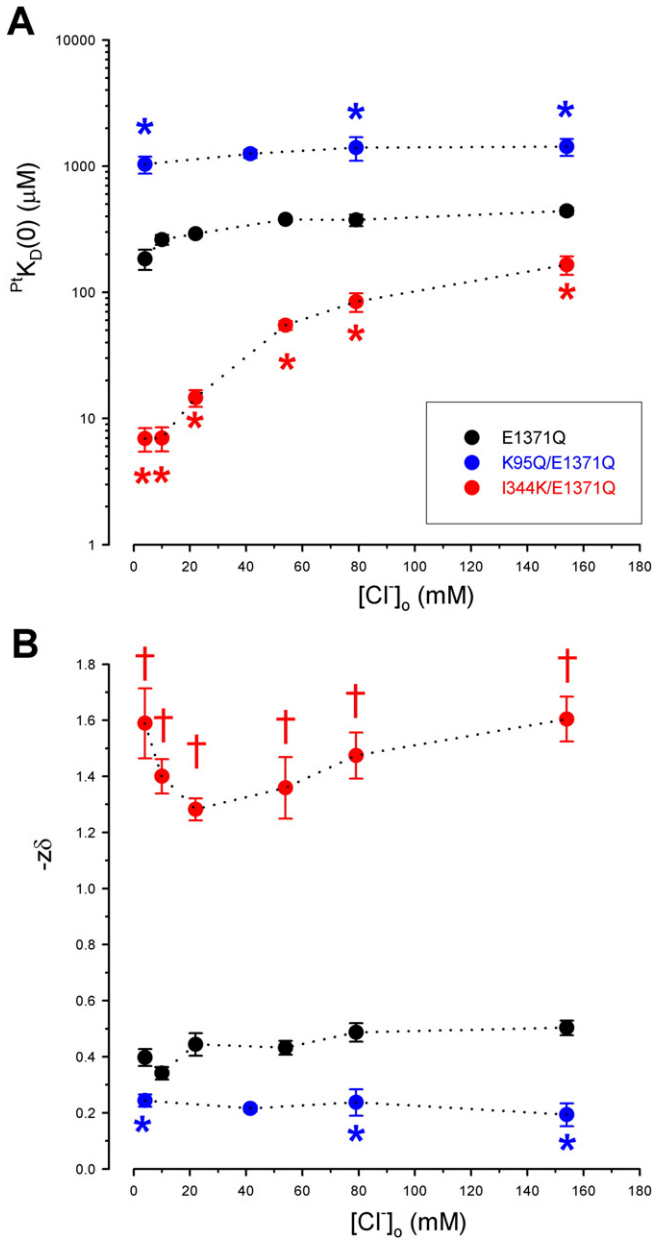

Fig. 5. Effect of mutations at the putative blocker binding site on $[Cl^-]$-dependence of block. (A) Relationship between $Pt(NO_2)_4^{2-}$ binding affinity ($^{Pt}K_D$ at 0 mV) and $[Cl^-]_o$ for E1371Q (black), K95Q/E1371Q (blue; see Fig. 1) and I344K/E1371Q (red; see Fig. 1). Asterisks indicate a significant difference from E1371Q ($P < 0.001$). (B) Relationship between blocker voltage dependence (zδ; obtained from fits such as those shown in Figs. 2G, 4D and 4I) and $[Cl^-]_o$ for these same channel variants. Asterisks and daggers indicate a significant difference from E1371Q (asterisks, $P < 0.005$; daggers, $P < 0.0000005$). Mean of data from three to nine patches.

when $Pt(NO_2)_4^{2-}$ enters the channel while the external Cl^- binding site is occupied there is significant coupling between the movement of $Pt(NO_2)_4^{2-}$ and Cl^- ions, leading to an increase in the apparent voltage dependence of the $Pt(NO_2)_4^{2-}$ binding reaction ($^{Pt}z\delta_{occ} > {}^{Pt}z\delta_{vac}$).

3.5. Quantitative analysis of anion binding in mutant channels

Similar analysis of Cl^--dependent $Pt(NO_2)_4^{2-}$ block in K95Q/E1371Q and I344K/E1371Q (Fig. 8B, C) provides additional insight into the effect of mutations close to the putative $Pt(NO_2)_4^{2-}$ binding site. The results of this analysis are summarized in Table 2. Compared to E1371Q, $Pt(NO_2)_4^{2-}$ binding was weakened in K95Q/E1371Q, both in Cl^--unoccupied (Fig. 8D) and Cl^--occupied channels (Fig. 8E), although its voltage dependence was little changed; and Cl^- binding itself was only slightly weakened (Fig. 8F). Since K95 is thought to play a dominant role in Cl^- binding in the inner vestibule [34,51,52], the finding that the K95Q mutation has only a small effect on Cl^- binding affinity is consistent with the hypothesis that external Cl^- is binding to a different site located in a more extracellular part of the channel. In fact, since $Pt(NO_2)_4^{2-}$ block is so weak in K95Q/E1371Q, the accuracy of estimated ^{Cl}K in this mutant is questionable. The I344K mutant has a profound impact on channel binding affinity of both intracellular $Pt(NO_2)_4^{2-}$ (Fig. 8D, E) and extracellular Cl^- (Fig. 8F) (summarized in Table 2). Compared to E1371Q, the intrinsic $Pt(NO_2)_4^{2-}$ binding affinity of I344K/E1371Q is increased ~1400-fold by the addition of a second fixed positive charge in the inner vestibule, with no apparent change in the voltage dependence of binding (Fig. 8D). Binding of $Pt(NO_2)_4^{2-}$ to Cl^--occupied channels is also stronger, and the voltage-dependence of binding ($^{Pt}z\delta_{occ}$) is approximately doubled (Fig. 8E), suggesting that coupling between the movement of $Pt(NO_2)_4^{2-}$ and Cl^- ions within the pore is greatly enhanced in this mutant. In fact, the impact of Cl^- binding on $Pt(NO_2)_4^{2-}$ binding affinity (the difference between $^{Pt}K_{vac}$ and $^{Pt}K_{occ}$) appears much greater in I344K/E1371Q than in E1371Q (Fig. 9). Finally, Cl^- binding affinity is higher in I334K/E1371Q (Fig. 8F; Table 2), suggesting that the I344K mutation strengthens interactions with external Cl^- ions as well as with internal $Pt(NO_2)_4^{2-}$ ions. Furthermore, the voltage-dependence of Cl^- binding is greatly increased, with $^{Cl}z\delta$ being increased >5-fold (Fig. 8F), suggesting that external Cl^- ions cross a much larger part of the transmembrane electric field to reach their binding site in this mutant.

External Cl^--dependence of $Pt(NO_2)_4^{2-}$ block is abolished in R334Q/E1371Q (Fig. 6C, D; Fig. 10A), consistent with the positive charge at this site in the outer vestibule of the pore (Fig. 1) being crucial for interactions between the channel and extracellular Cl^- ions that are required for ion:ion interactions inside the pore [33,43]. Binding of $Pt(NO_2)_4^{2-}$ ions to R334Q/E1371Q was somewhat weaker than E1371Q (Fig. 10C; Table 2), consistent with earlier reports that mutations at R334 disrupt blocker binding in the pore inner vestibule, perhaps by a long-range conformational effect on the pore [56]. The voltage-dependence of $Pt(NO_2)_4^{2-}$ binding is also increased in R334Q/E1371Q (Fig. 10C). However, the very low apparent Cl^- affinity of R334Q/E1371Q implied by the apparent $[Cl^-]$-independence of $^{Pt}K_D$ in this mutant (Figs. 6D, 10A) precluded quantitative analysis of $^{Pt}K_{occ}(0)$ and ^{Cl}K in this case; the lack of slope illustrated in the relationships in Figs. 6D and 10A imply extremely low Cl^- binding affinity, consistent with ablation of the external Cl^- binding site.

Although the R334Q mutant abolished Cl^--dependence of $Pt(NO_2)_4^{2-}$ block, the double pore mutant R334Q/I344K/E1371Q showed strongly Cl^--dependent block (Fig. 6E–H; Fig. 10B), suggesting that the presence of the I344K mutant restores Cl^- binding that is lost in R334Q/E1371Q. Quantitative analysis of data from R334Q/I344K/E1371Q (Fig. 10; Table 2) suggests that the presence of the second fixed positive charge in the inner vestibule at position 344 still supports strong $Pt(NO_2)_4^{2-}$ binding (Fig. 10C), although (as for E1371Q) $Pt(NO_2)_4^{2-}$ binding is somewhat weakened by the R334Q mutation (Fig. 10C). Binding of $Pt(NO_2)_4^{2-}$ to Cl^--occupied channels is similar in R334Q/E1371Q and R334Q/I344K/E1371Q (Fig. 10D), suggesting that R334 plays little or no role in ion:ion interactions in mutant channels bearing a positive charge at position 344. Chloride binding also remains strong in R334Q/I344K/E1371Q, although it too is somewhat weakened by the R334Q mutation (Fig. 10E). The strong effect of external Cl^- on $Pt(NO_2)_4^{2-}$ binding to R334Q/I344K/E1371Q channels is illustrated in Fig. 9D.

Because the effect of external SCN^- on $Pt(NO_2)_4^{2-}$ block was so dramatically altered in I344K/E1371Q (Fig. 7C, E, G), quantitative analysis of the effects of SCN^- was also carried out (Fig. 11; Table 3). As for external Cl^- (Fig. 8), there was a linear relationship between $[SCN^-]_o$ and $^{Pt}K_D$, both in E1371Q (Fig. 11A) and I344K/E1371Q (Fig. 11E), consistent with competition between SCN^- and $Pt(NO_2)_4^{2-}$ ions. In I344K/

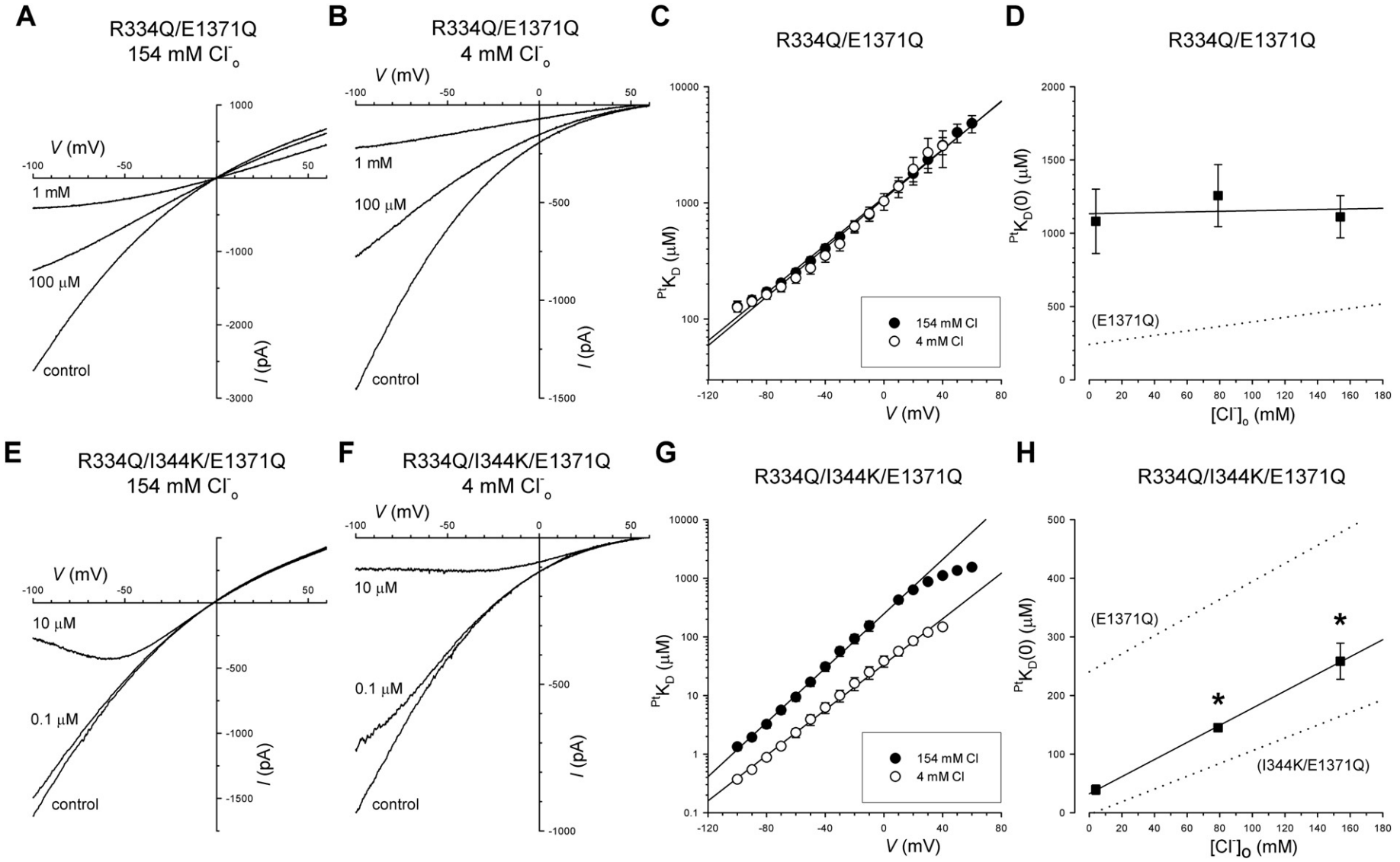

Fig. 6. Effect of mutations at a putative extracellular anion binding site on block by intracellular $Pt(NO_2)_4^{2-}$. (A, B, E, F) Example macroscopic *I–V* relationships for R334Q/E1371Q (A, B) or R334Q/I344K/E1371Q (E, F) under high (154 mM; A, E) or low (4 mM; B, F) extracellular [Cl^-] conditions. In each case currents were recorded before (control) and after the addition of $Pt(NO_2)_4^{2-}$ (at the concentrations indicated) to the intracellular solution. (C, G) Mean $^{Pt}K_D$ values for these channel variants at different membrane potentials, obtained and fitted as described in Figs. 2 and 4. (D, H) Mean values of $^{Pt}K_D$ at 0 mV membrane potential obtained from fits of $^{Pt}K_D$–*V* relationships to Eq. (2) at different extracellular [Cl^-]. Asterisks indicate a significant difference from 4 mM Cl^-_o ($P < 0.0005$). There was no significant difference in these parameters for R334Q/E1371Q (E) ($P > 0.5$). Dotted lines indicate the fit to data for E1371Q (see Fig. 2H) or I344K/E1371Q (see Fig. 4J) as indicated. Mean of data from three to five patches.

E1371Q, ^{SCN}K was greatly reduced (Fig. 11F; Table 3), $^{Pt}K_{occ}(0)$ was slightly increased (Fig. 11G; Table 3), and both $^{SCN}z\delta$ and $^{Pt}z\delta_{occ}$ were increased (Fig. 11F, G; Table 3). In both E1371Q (Fig. 11D) and I344K/E1371Q (Fig. 11H), SCN^- binding had a greater destabilizing impact on $Pt(NO_2)_4^{2-}$ binding than did Cl^-.

3.6. Effect on single channel conductance

The results in Figs. 6 and 7 suggest that antagonistic ion:ion interactions inside the pore that are lost following removal of the positive charge at R334 are at least partially restored by the I344K mutation. These interactions may be important for maximization of single channel conductance (see Introduction), as exemplified by the very low conductance observed for R334Q and for other substitutions at this site [33]. However, the reduced single channel conductance observed in R334Q channels (Fig. 12) was not significantly rescued by the I344K mutation (Fig. 12). This contrasts with the previous observation that the I344K mutation, while having little influence on single channel conductance by itself, could almost completely restore the greatly diminished conductance seen when K95 in the inner vestibule is neutralized by mutagenesis [50]. In other words, in terms of single channel conductance, introduction of a positively charged lysine at position I344 is able to compensate for the loss of a native positive charge in the inner vestibule [50] but not in the outer vestibule (Fig. 12).

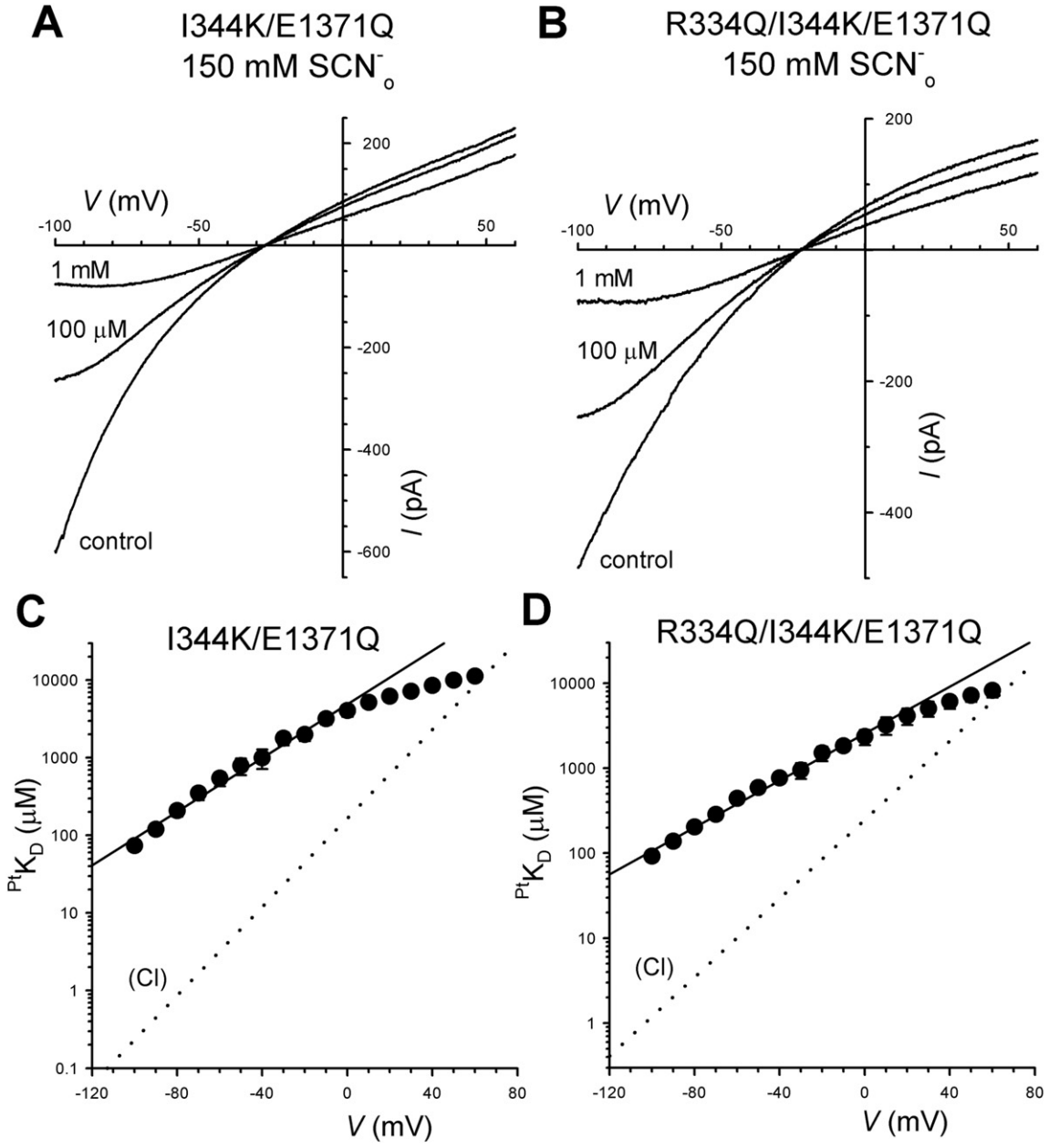

Fig. 7. Effect of other extracellular anions on $Pt(NO_2)_4^{2-}$ block of I344K-containing channels. (A, B) Example macroscopic *I–V* relationships for I344K/E1371Q (A) or R334Q/I344K/E1371Q (B) with extracellular solution containing 150 mM SCN^-. Currents were recorded before (control) and after the addition of 100 μM and 1 mM $Pt(NO_2)_4^{2-}$ to the intracellular solution. (C, D) Mean $^{Pt}K_D$ values for these channel variants at different membrane potentials under these ionic conditions, obtained and fitted as described in Figs. 2 and 4. (E, F) Mean values of $^{Pt}K_D$ at 0 mV membrane potential obtained from fits of $^{Pt}K_D$–*V* relationships using Eq. (2) at different extracellular [SCN^-]. Dotted lines indicate the fit to data for the same channel variants as a function of extracellular [Cl^-] (see Figs. 4J and 6H) as indicated. (G, H) Mean values of $^{Pt}K_D$ at 0 mV when the extracellular solution contained 150 mM of the different anions indicated. Asterisks indicate a significant difference from gluconate and daggers indicate a significant difference from Cl^- ($P < 0.05$). Mean of data from three to four patches.

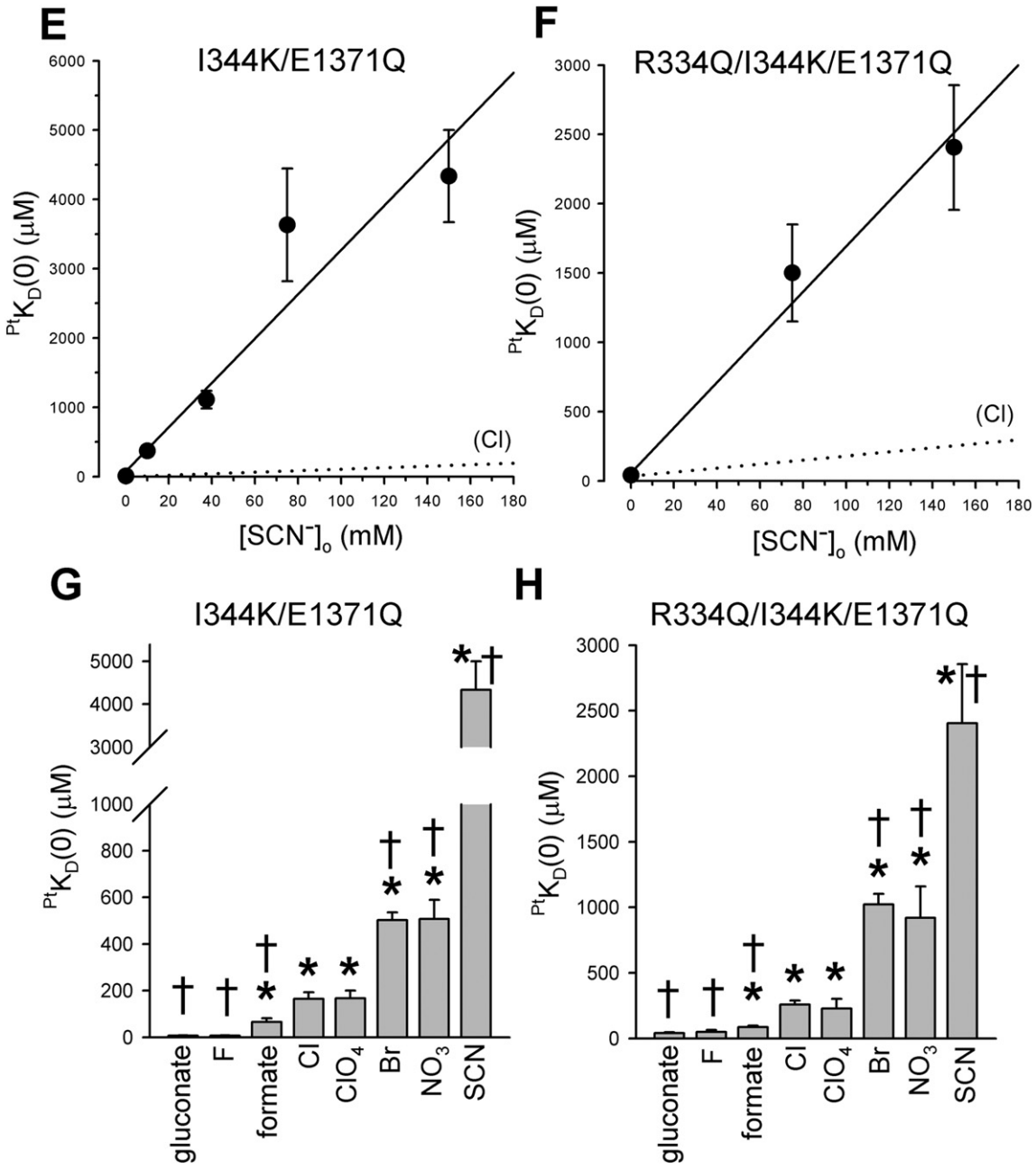

Fig. 7 (*continued*).

4. Discussion

4.1. Isolating Cl^-:blocker interactions inside the CFTR pore

The CFTR channel is subject to block by many different cytoplasmic anions that bind within its inner vestibule and interact with the positive charge of K95 [35,51]. In many cases, this blocking action has been described as being antagonized by extracellular Cl^- ions [28–30,36–41]. It has been proposed that this antagonism allows some level of physiological regulation of CFTR function by extracellular Cl^- ions, which may increase overall CFTR function by weakening block by endogenous cytoplasmic anions during periods of epithelial Cl^- secretion [41]. In fact, extracellular Cl^- ions have been proposed to interact with cytoplasmic blocking anions by two distinct molecular mechanisms, one involving Cl^- binding inside the pore and the other resulting from Cl^- interaction with a site outside the pore on the extracellular face of the protein [35] (Fig. 1). The present study using constitutively active E1371Q channels appears to effectively isolate the effects of Cl^- acting inside the pore, at least for the test blocker $Pt(NO_2)_4^{2-}$. Thus, block by cytoplasmic $Pt(NO_2)_4^{2-}$ ions — and its dependence on extracellular [Cl^-] — is independent of the R899Q mutation (in an E1371Q background) (Fig. 2; Table 1). This R899Q mutation has previously been shown to disrupt the antagonistic effects of Cl^- and other extracellular anions on block by different cytoplasmic anions, including $Pt(NO_2)_4^{2-}$ [45,46]. The present results therefore suggest that any effects of extracellular Cl^- on channel block that are mediated via interaction with R899 are not the result of a change in blocker interactions with the open channel pore. Instead, these R899-mediated effects may reflect a more indirect effect of extracellular Cl^-. For example, extracellular [Cl^-] has been shown to affect CFTR channel gating, leading to a higher channel open probability at higher [Cl^-], and this effect of Cl^- is thought to result from an interaction with R899 on the extracellular face of the protein [53]. Since

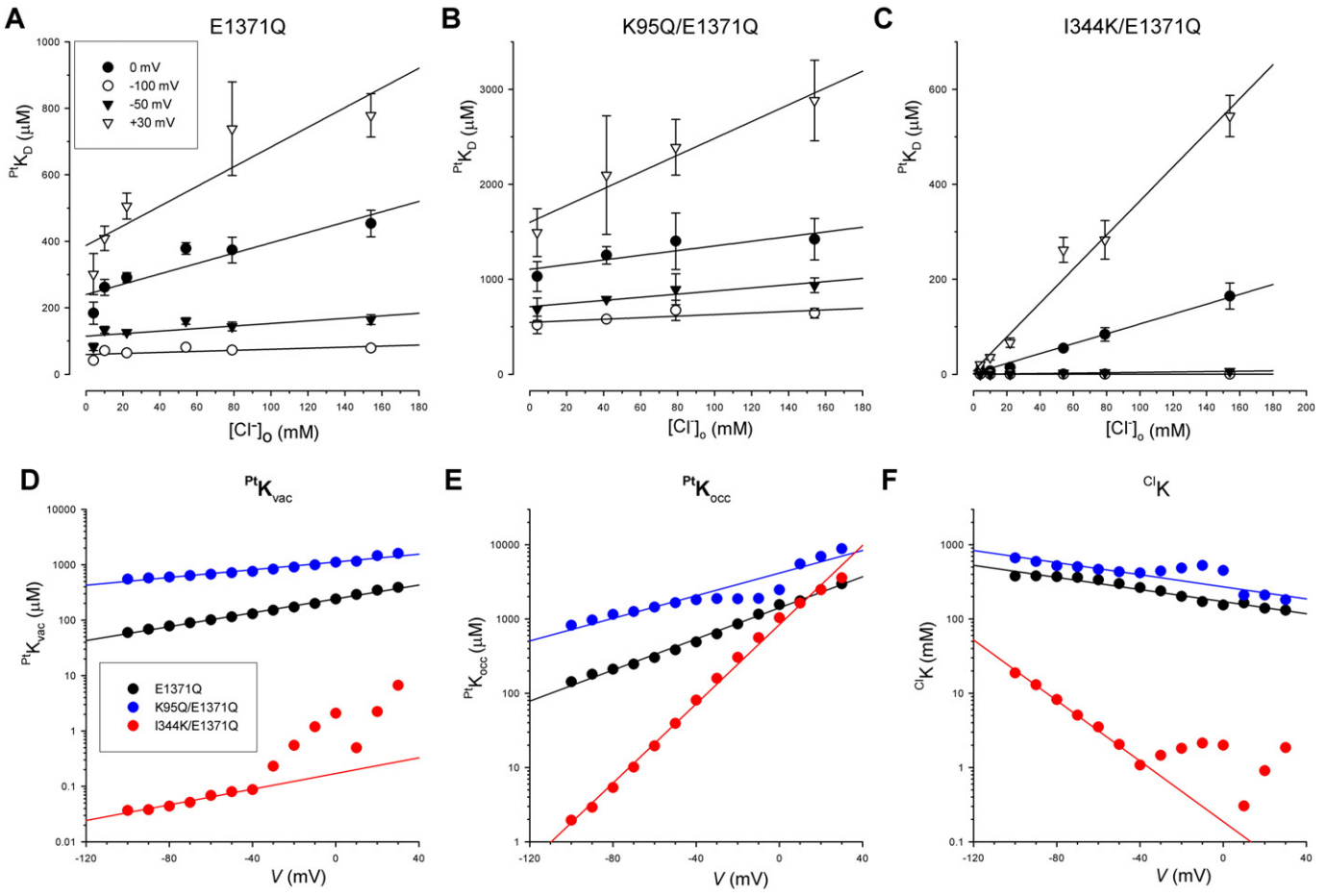

Fig. 8. Analysis of the Cl^--dependence of $Pt(NO_2)_4^{2-}$ block in channel variants with altered $Pt(NO_2)_4^{2-}$ binding. (A–C) Effect of extracellular [Cl^-] ($[Cl^-]_o$) on the measured $^{Pt}K_D$ in E1371Q (A), K95Q/E1371Q (B) and I344K/E1371Q (C) at different membrane potentials as indicated in panel A. Straight-line fits to the data are to Eq. (3) as described in the Materials and methods. Mean of data from three to nine patches. (D–F) Values of $^{Pt}K_{vac}$ (D; a measure of the dissociation constant for $Pt(NO_2)_4^{2-}$ binding to channels when the external Cl^- binding site is vacant), $^{Pt}K_{occ}$ (E; a measure of the dissociation constant for $Pt(NO_2)_4^{2-}$ binding to channels when the external Cl^- binding site is occupied) and ^{Cl}K (F; a measure of the dissociation constant for extracellular Cl^- binding to the external binding site) for these three channel variants. These values were obtained from individual fits by Eq. (3) to mean data as shown in A–C, as described in the Materials and methods. Straight line fits to the data in (D–F) were used to obtain the values for $^{Pt}z\delta_{vac}$, $^{Pt}z\delta_{occ}$ and $^{Cl}z\delta$ given in Table 2, as described in the Materials and methods. Data for I344K/E1371Q at positive voltages appear unreliable, likely due to the very strong voltage dependence of block observed in this mutant.

block by intracellular $Pt(NO_2)_4^{2-}$ is also gating state-dependent [47], this could result in an indirect Cl^--dependence of $Pt(NO_2)_4^{2-}$ block. For example, increasing extracellular [Cl^-], by increasing channel open probability, could reduce the ability of $Pt(NO_2)_4^{2-}$ to interact with and stabilize the closed state of the channel [47], leading to a reduction of its overall apparent blocking potency under high $[Cl^-]_o$ conditions.

Table 2
Mean parameters obtained from analysis of the $[Cl^-]_o$-dependence of $Pt(NO_2)_4^{2-}$ block in different channel variants, as described in Figs. 8 and 10. Because of the lack of $[Cl^-]_o$-dependence in R334Q/E1371Q, values for $^{Pt}K_{occ}$, $^{Pt}z\delta_{occ}$, ^{Cl}K and $^{Cl}z\delta$ could not be obtained for this mutant.

	$^{Pt}K_{vac}(0)$ (μM)	$^{Pt}z\delta_{vac}$	$^{Pt}K_{occ}(0)$ (μM)	$^{Pt}z\delta_{occ}$	^{Cl}K (mM)	$^{Cl}z\delta$
E1371Q	245	−0.39	1440	−0.63	179	+0.22
K95Q/E1371Q	1150	−0.23	4400	−0.58	296	+0.20
I344K/E1371Q	0.174	−0.42	978	−1.12	0.264	+1.09
R334Q/E1371Q	1120	−0.71	–	–	–	–
R334Q/I344K/E1371Q	31.8	−1.04	1500	−1.15	232	+0.23

4.2. The mechanism of knock-off

The multiple effects of extracellular [Cl^-] on CFTR channel block by cytoplasmic anions may have obscured earlier attempts to identify important anion binding sites in the pore, as well as the nature of ion–ion interactions occurring inside the pore. The ability of the E1371Q background effectively to isolate antagonistic interactions between external anions and intracellular $Pt(NO_2)_4^{2-}$ blocking anions that occur inside the open channel pore affords a novel opportunity to investigate the nature and molecular bases of these antagonistic interactions. The present results suggest a competitive interaction between intracellular $Pt(NO_2)_4^{2-}$ and extracellular Cl^- when these two anions are bound to separate sites inside the pore (Fig. 13A). As with other cytoplasmic blockers [35], $Pt(NO_2)_4^{2-}$ binds in the inner vestibule and interacts with the positive charge of K95 [47,48] (Figs. 4, 5, 8; Table 1). Addition of a second positive charge in the inner vestibule in I344K strengthens $Pt(NO_2)_4^{2-}$ binding (Figs. 4, 5, 8; Table 1), consistent with this residue also existing close to the internal blocker binding site [35,50] (Fig. 13A). External Cl^- binding requires a positive charge at R334 (Fig. 6) as suggested previously [31,43,48]. Conversely, removing the positive charge at K95 had only a minor effect on external Cl^- binding (Fig. 8F; Table 2), consistent with these two crucial positively charged residues contributing to separate anion binding sites (Figs. 1, 13A).

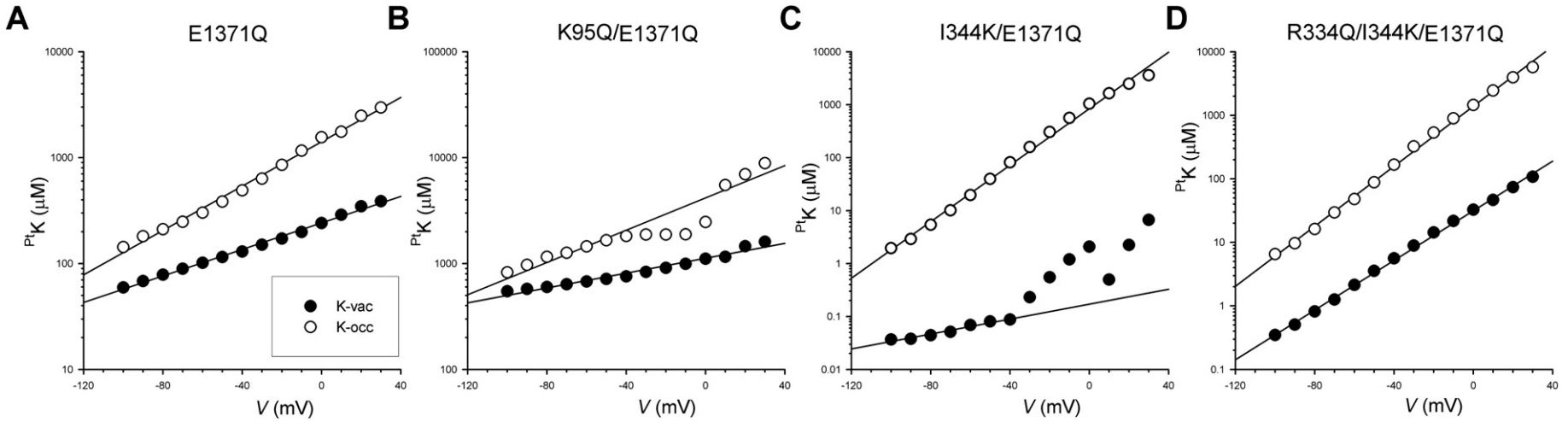

Fig. 9. Effect of bound extracellular Cl^- ions on the binding of intracellular $Pt(NO_2)_4^{2-}$ ions. Values of $^{Pt}K_{vac}$ and $^{Pt}K_{occ}$, obtained as described in Figs. 8 and 10, are compared for each of the four named channel variants. As noted in the legend to Fig. 8, data for I344K/E1371Q at positive voltages appear unreliable, likely due to the very strong voltage dependence of block observed in this mutant.

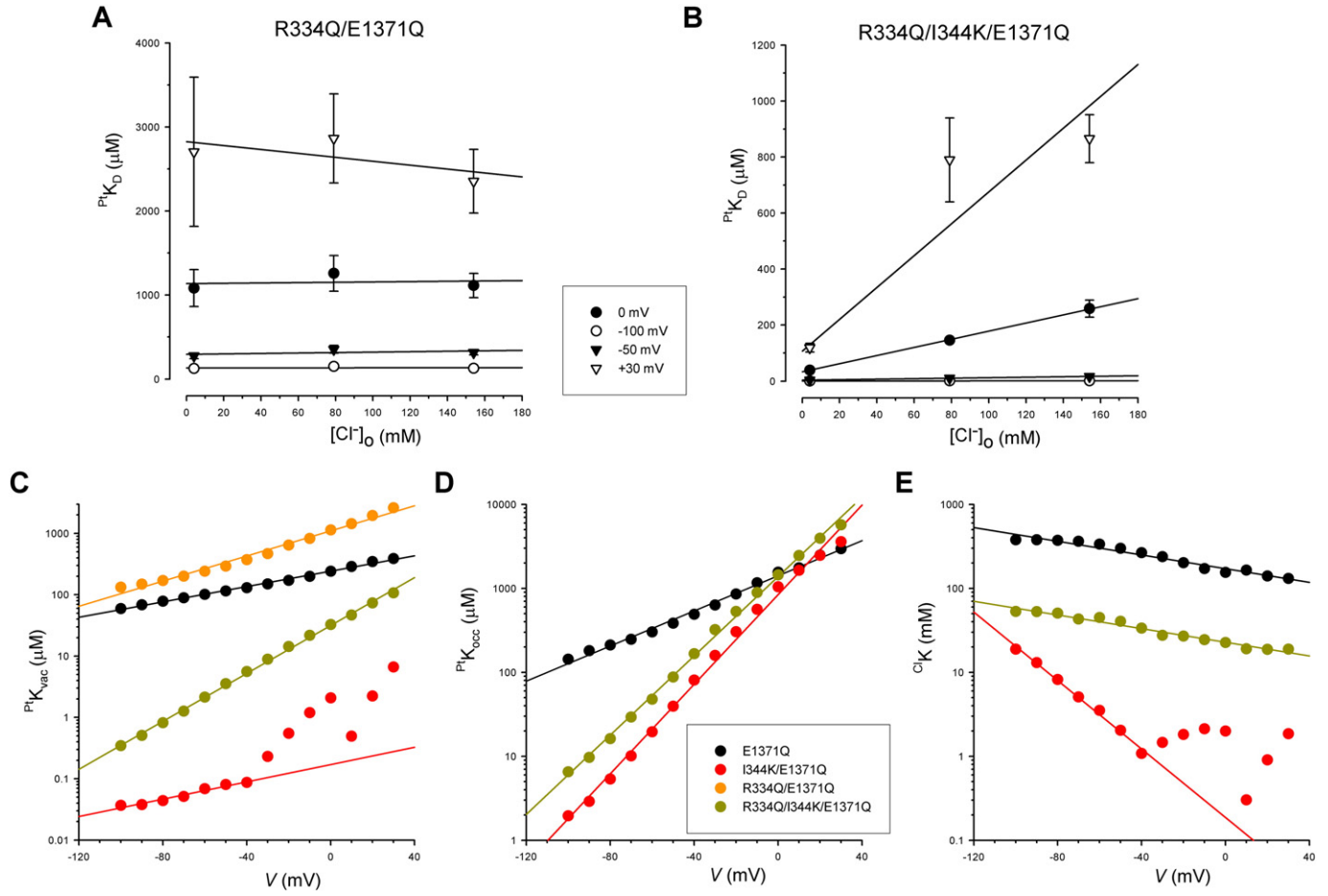

Fig. 10. Analysis of $Pt(NO_2)_4^{2-}$ and Cl^- binding to channel variants containing the R334Q mutation. (A, B) Effect of extracellular $[Cl^-]$ ($[Cl^-]_o$) on the measured $^{Pt}K_D$ in R334Q/E1371Q (A) and R334Q/I344K/E1371Q (B) at different membrane potentials as indicated. Straight-line fits to the data by Eq. (3) are as described in Fig. 8. Mean of data from three to five patches. (C–E) Values of $^{Pt}K_{vac}$ (D), $^{Pt}K_{occ}$ (E) and ^{Cl}K (F) for different channel variants as indicated. Note that, because of the apparent lack of effect of external Cl^- on $Pt(NO_2)_4^{2-}$ block in R334Q/E1371Q, it was not possible to obtain values for $^{Pt}K_{occ}$ or ^{Cl}K for this mutant. Straight line fits to the data by Eq. (3) were used to obtain the values for $^{Pt}z\delta_{vac}$, $^{Pt}z\delta_{occ}$ and $^{Cl}z\delta$ given in Table 2, as described in the Materials and methods. As noted in the legend to Fig. 8, data for I344K/E1371Q at positive voltages appear unreliable, likely due to the very strong voltage dependence of block observed in this mutant.

Both $Pt(NO_2)_4^{2-}$ binding and Cl^- binding are voltage-dependent (Fig. 8; Table 2), suggesting that both the internal and external binding sites are located within the transmembrane electric field (Fig. 13A).

Binding of $Pt(NO_2)_4^{2-}$ to the inner site is weakened when Cl^- (or other anions) are bound to the outer site (Fig. 9; Table 2), suggesting that external anions can "knock off" anions bound to the internal site (Fig. 13A). Furthermore, the increased voltage-dependence of $Pt(NO_2)_4^{2-}$ binding to Cl^--occupied channels (Fig. 8D, E; Fig. 9C; Table 2) is consistent with coupled movement between these two ions in the pore as described previously [30], in which $Pt(NO_2)_4^{2-}$ entry into the pore from the inside occurs in concert with Cl^- exit to the outside. Classical models of knock-off in ion channel pores involve repulsive electrostatic interactions between ions bound concurrently to nearby sites [13,21,42], and it may be that Cl^- and $Pt(NO_2)_4^{2-}$ ions experience direct electrostatic interactions within the pore. However, the proposed locations of the two putative anion binding sites — in the inner and outer vestibules respectively (Fig. 1) — might be expected to limit the potential for direct electrostatic interactions between anions bound to these sites (although it is possible that ions bound to distant sites may experience indirect electrostatic interactions mediated *via* knock-on of ions bound to other, intervening sites). Alternatively, anion binding to one site may reduce anion binding affinity at the other site via a conformational change in the channel protein. For example, in K^+ channel pores it has been proposed that ion binding to one site in the pore alters the affinity for ion binding to other sites due to a propagated conformational rearrangement [59,62]. Consistent with the idea that inner and outer anion binding sites are conformationally linked, mutations at R334 have been shown to lead to a change in the affinity of blocker binding in the inner vestibule for anions that interact directly with K95 [48]. Indeed, the R334Q mutation significantly decreases $Pt(NO_2)_4^{2-}$ binding affinity (Fig. 10C; Table 1). Present results also suggest that the K95Q mutation causes a small decrease in the Cl^- binding affinity of the outer site (Fig. 8F; Table 2).

Other extracellular anions (ClO_4^-, Br^-, NO_3^-, SCN^-) exert a stronger antagonistic effect on internal $Pt(NO_2)_4^{2-}$ block than does Cl^- (Fig. 3), suggesting that they may bind more tightly to the external anion binding site, while F^- and formate have no apparent impact on $Pt(NO_2)_4^{2-}$ binding (Fig. 3), suggesting they may bind only weakly if at all to the external site. Indeed, the apparent affinity for extracellular SCN^- (Fig. 11B; Table 3) was >12-fold greater than for Cl^- (Fig. 8F; Table 2). As suggested previously [30], the external anion binding site may show lyotropic anion selectivity, binding lyotropic anions with low free energy of hydration (such as SCN^-) with higher affinity than kosmotropic anions with high free energy of hydration (such as F^-).

4.3. A second mechanism of knock-off in I344K-containing channel pores

Addition of a second positive charge lining the inner vestibule in I344K/E1371Q increases intrinsic $Pt(NO_2)_4^{2-}$ binding affinity ~1400-fold (Figs. 5, 8; Table 2), likely because the additional positive charge increases electrostatic interactions with divalent $Pt(NO_2)_4^{2-}$ anions [47] (Fig. 13B). However, this I344K mutation also has a strong influence

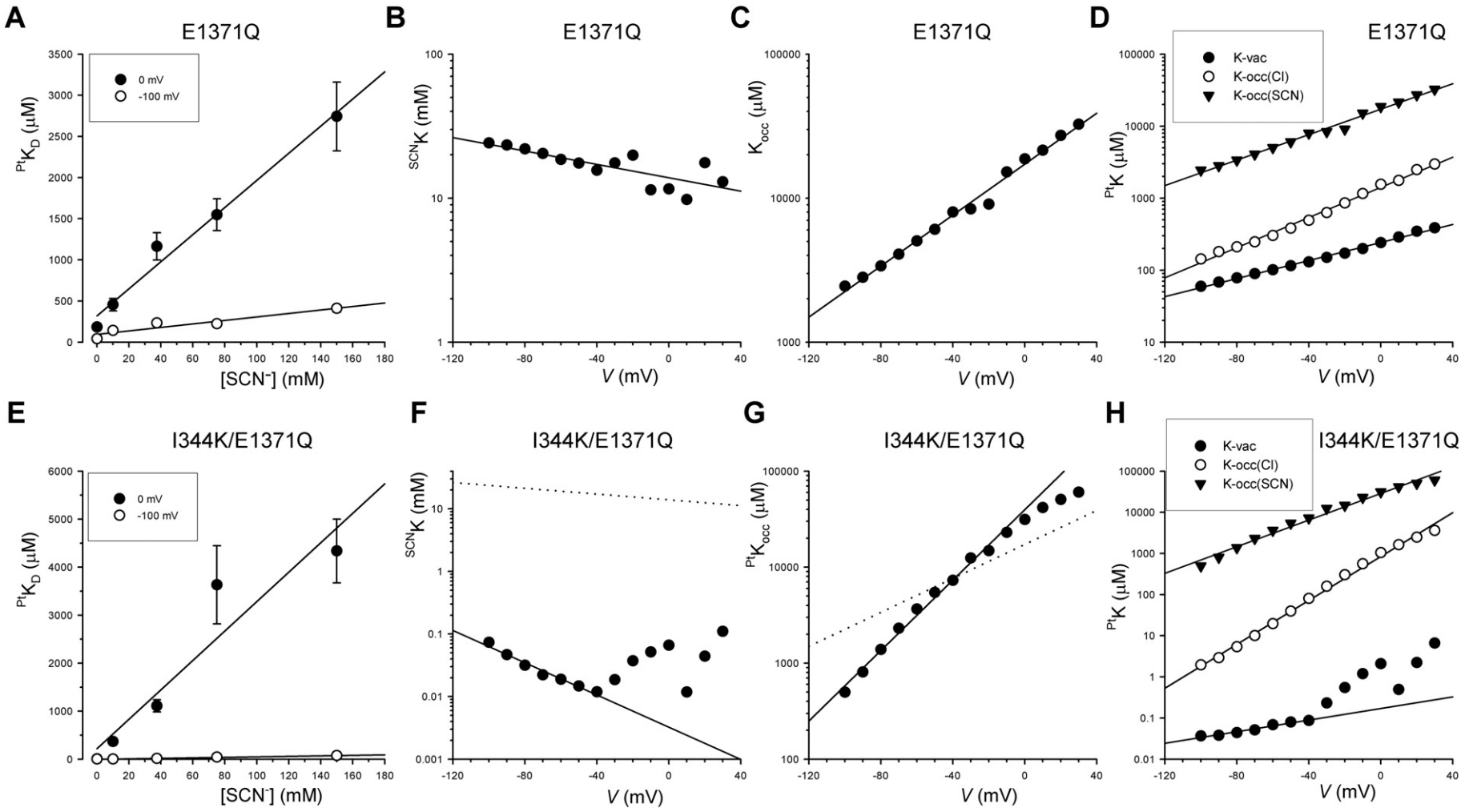

Fig. 11. Analysis of the SCN^--dependence of $Pt(NO_2)_4^{2-}$ block. (A, E) Effect of extracellular [SCN^-] ([SCN^-]$_o$) on the measured $^{Pt}K_D$ in E1371Q (A) and I344K/E1371Q (E) at 0 mV and −100 mV membrane potential. Straight-line fits to the data are as described in the Materials and methods. Mean of data from three to six patches. (B,C,F,G) Values of ^{SCN}K and $^{Pt}K_{occ}$ for these two channel variants. These values were obtained from individual fits to mean data as shown in A and E, as described in the Materials and methods. Straight line fits to the data in B, C, F, and G were used to obtain the values for $^{SCN}z\delta$ and $^{Pt}z\delta_{occ}$ given in Table 3, as described in the Materials and methods. Dotted lines in F and G indicate the fit to data for E1371Q (from B and C). As noted in the legend to Fig. 8, data for I344K/E1371Q at positive voltages appear unreliable, likely due to the very strong voltage dependence of block observed in this mutant. (D, H) Comparison of ^{Pt}K values estimated under different conditions — external site vacant (K-vac), external site occupied by Cl^- (K-occ(Cl)) and external site occupied by SCN^- (K-occ(SCN)) — as described in C and G and Fig. 8.

Table 3
Mean parameters obtained from analysis of the $[SCN^-]_o$-dependence of $Pt(NO_2)_4^{2-}$ block in E1371Q and I344K/E1371Q, as described in Fig. 11. Note that $^{Pt}K_{vac}(0)$ and $^{Pt}z\delta_{vac}$ are independent of the extracellular anion, since they refer to channels in which the external anion binding site is vacant.

	$^{Pt}K_{occ}(0)$ (μM)	$^{Pt}z\delta_{occ}$	^{SCN}K (μM)	$^{SCN}z\delta$
E1371Q	17,500	−0.54	14,000	+0.137
I344K/E1371Q	32,900	−0.94	1.95	+0.917

on binding of external Cl^- ions, increasing Cl^- binding affinity and also increasing the voltage-dependence of Cl^- binding (Fig. 8F; Table 2). Binding of external SCN^- ions was even more strongly affected, with apparent SCN^- affinity increased >7000-fold, again with a >6-fold increase in voltage-dependence of SCN^- binding (Fig. 11; Table 3). These two effects on binding of internal $Pt(NO_2)_4^{2-}$ and external anions suggest that the I344K mutation alters, directly or indirectly, ion interactions with two different binding sites inside the pore. The alternative to this — that I344K increases the anion binding affinity of a single site that interacts with both internal $Pt(NO_2)_4^{2-}$ and external Cl^- — can be ruled out based on the shape of the $^{Pt}K_D$–$[Cl^-]_o$ relationship for this mutant (Fig. 4J). This relationship almost passes through the origin (giving an exquisitely low value for $^{Pt}K_{vac}$) even though these experiments were carried out under constant high intracellular $[Cl^-]$ conditions (154 mM Cl^-). If $Pt(NO_2)_4^{2-}$ and Cl^- were competing for a single binding site in these experiments, then intracellular Cl^- should be just as effective as extracellular Cl^- in weakening $Pt(NO_2)_4^{2-}$ block. Consequently, if we assume that the I344K mutation is increasing the affinity of a Cl^- binding site on the extracellular side of the $Pt(NO_2)_4^{2-}$ binding site, then this could reflect an increase in the Cl^--binding affinity of the "normal" Cl^- binding site in the outer vestibule, or the introduction of a novel Cl^- binding site elsewhere in the pore. Several findings of the present study support the second of these two hypotheses. Mutating a key positive charge in the outer vestibule (R334) abolishes Cl^--dependence of block (Fig. 6), likely by disrupting the external Cl^- binding site (Fig. 13A, B). However, the R334Q mutation has only a minor impact on Cl^- binding in the presence of I344K, and Cl^- binding to the R334Q/I344K/E1371Q mutant remains strong and strongly voltage-dependent (Fig. 10; Table 2). This suggests that in I344K-containing channels (unlike E1371Q background channels), significant binding of extracellular Cl^- occurs at a site that is independent of R334. Indeed, knock-off of $Pt(NO_2)_4^{2-}$ by Cl^- appears similar in I344K/E1371Q and R334Q/I344K/E1371Q channels (Fig. 10D), suggesting that anion binding near R334 plays little role in ion:ion interactions that occur in channels bearing the I344K mutation. Furthermore, the voltage-dependence of external Cl^- binding is greatly increased in I344K-containing channels. While estimated zδ values have no direct physical meaning, and the relationship between the transmembrane electric field and physical distance is not straightforward, this increased voltage dependence could be considered consistent with external Cl^- ions penetrating further into the pore from its extracellular end to interact with $Pt(NO_2)_4^{2-}$ ions bound in the inner vestibule (Fig. 13B). The apparent anion selectivity of the external anion binding site is also slightly altered in I344K-containing channels (Fig. 7G, H), and this appears independent of the presence or absence of the R334Q mutation. Not only the binding affinity of external Cl^- and internal $Pt(NO_2)_4^{2-}$, but also the

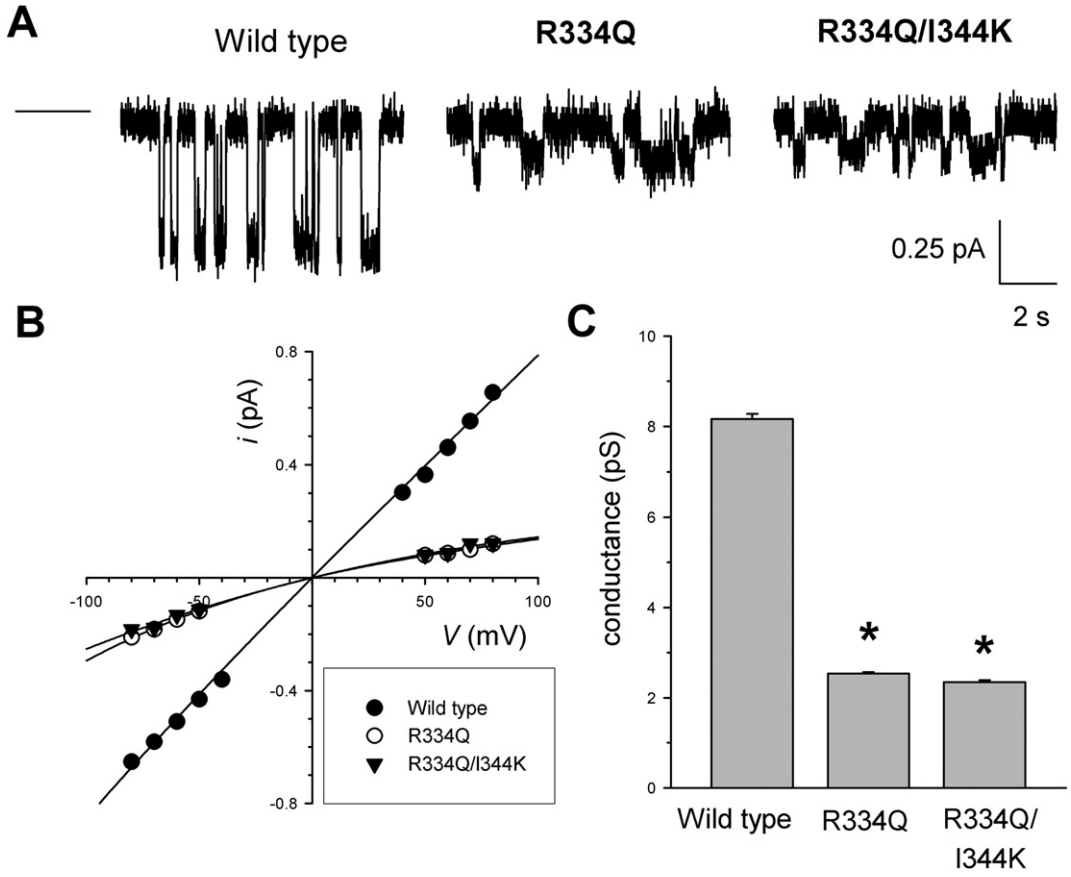

Fig. 12. Single channel conductance of R334Q-containing channels. (A) Example single-channel currents recorded at a membrane potential of −60 mV for the wild type, R334Q, and R334Q/I344K channels as indicated. The channel closed state is indicated by the line to the left. (B) Mean single channel *I–V* relationships for these three channel variants. (C) Mean single channel conductance measured at hyperpolarized membrane potentials for these channel variants. Mean of data from six to ten patches. Asterisks indicate a significant difference from wild type conductance ($P < 10^{-10}$).

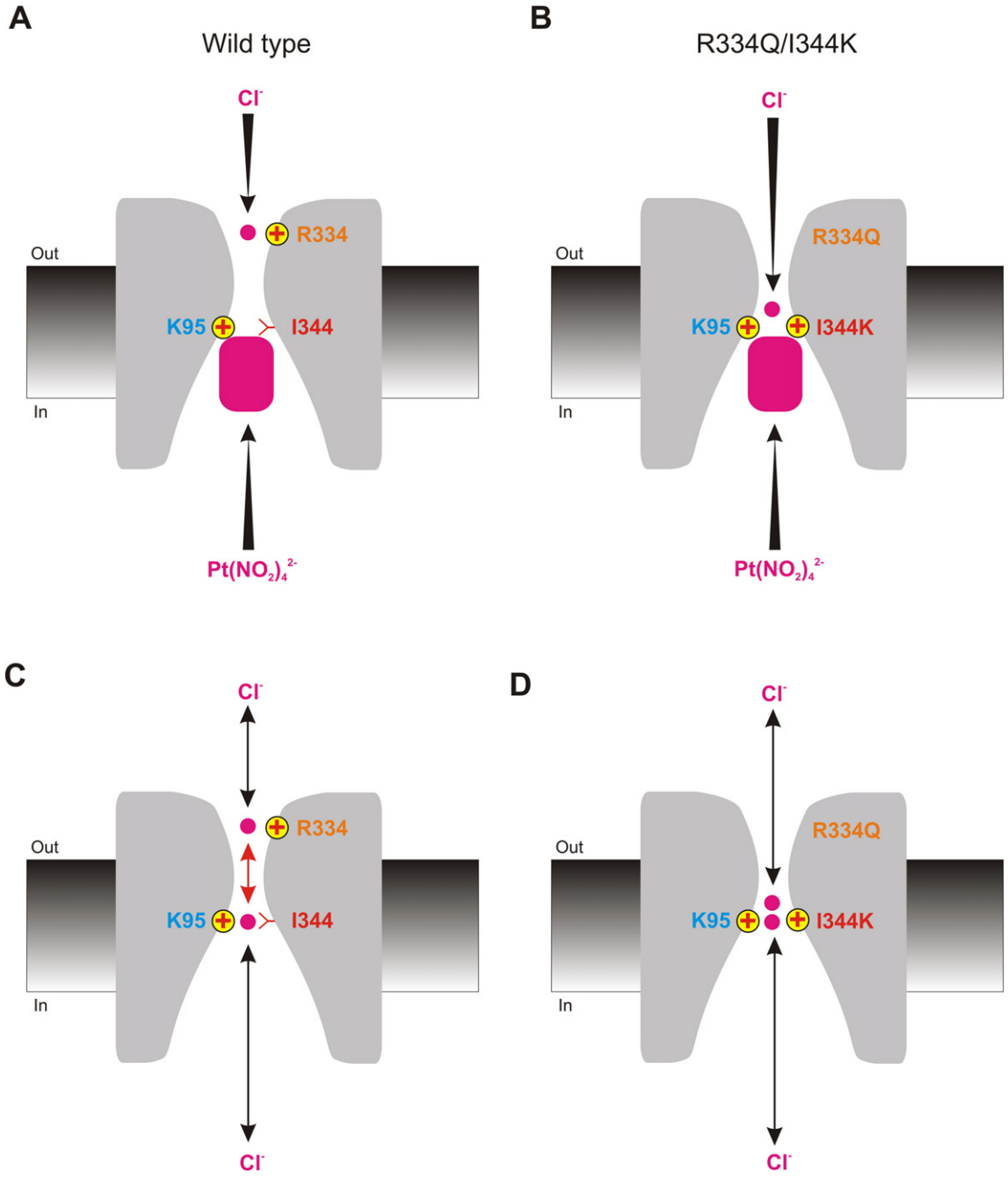

Fig. 13. Cartoon models of different proposed ion:ion interactions occurring within the pore. Different models depict different ion:ion interactions underlying knock-off of intracellular $Pt(NO_2)_4^{2-}$ ions by extracellular Cl^- (A, B) and repulsive Cl^-:Cl^- interactions that might occur during Cl^- permeation (C, D). These different mechanisms are illustrated in wild type (A, C) and R334Q/I344K channels (B, D) that are proposed to isolate the two different mechanisms of ion:ion interaction; it is presumed that both mechanisms are active in I344K (and neither in R334Q). (A) In wild type CFTR, binding of Cl^- near the outer mouth of the pore (close to R334) antagonizes binding of $Pt(NO_2)_4^{2-}$ within the inner vestibule (close to K95 and I344). (B) In R334Q/I344K channels, Cl^- does not bind to the outer pore mouth, but instead binds further into the pore from its extracellular end (experiencing a greater fraction of the transmembrane electric field) and binds close to the introduced lysine in the inner vestibule, where it strongly antagonizes $Pt(NO_2)_4^{2-}$ binding (leading to very strong $[Cl^-]_o$-dependence of block). (C) In wild type, mutually antagonistic binding of Cl^- ions to relatively distant sites (red arrow) ensures rapid throughput of Cl^- ions, increasing overall Cl^- conductance. (D) In R334Q/I344K, even if multiple Cl^- ions are able to bind close together in the inner vestibule, this does not result in rapid Cl^- permeation in the absence of Cl^- binding to the outer pore region. This model suggests that the relative location of Cl^- binding sites, and not just the presence of multiple binding sites that are capable of experiencing mutually antagonistic binding, is required to maximize Cl^- conductance.

strength of the interaction between them, is altered in I344K-containing channels. Thus, the destabilizing effect of Cl^- on $Pt(NO_2)_4^{2-}$ binding — evaluated from the difference between $Pt(NO_2)_4^{2-}$ binding in vacant and Cl^--occupied channels (i.e. between $^{Pt}K_{vac}$ and $^{Pt}K_{occ}$) — is much greater in I344K/E1371Q (and to a lesser extent R334Q/I344K/E1371Q) than in E1371Q or K95Q/E1371Q (Fig. 9). Strengthened interactions between bound anions are also suggested by the increased apparent coupling between the movement of $Pt(NO_2)_4^{2-}$ and Cl^- ions inside the pore in I344K (Fig. 8E).

One model that appears consistent with these results is that addition of a second positive charge in the inner vestibule (in I344K/E1371Q) increases the number of anions that can bind within this region of the pore (Fig. 13B). Mutual destabilization between anions bound to these

nearby sites could then introduce a novel, strongly destabilizing effect of external Cl^- on internal $Pt(NO_2)_4^{2-}$ binding in I344K-containing channels. This model is in some ways reminiscent of the selectivity filter of voltage-dependent Ca^{2+} channels, that use charged amino acid side chains to bind one Ca^{2+} ion very tightly or can accommodate two Ca^{2+} ions simultaneously at very much reduced affinity [14]. Furthermore, because this destabilizing effect involves local interactions between bound anions (Fig. 13B), it may be relatively independent of anion binding in the outer vestibule of the pore — close to R334, which is required for normal anion:anion interactions observed in E1371Q background channels (Fig. 13A). Chloride ions entering the pore from its extracellular end are able to bind much deeper inside the pore — potentially increasing the voltage-dependence of the Cl^- binding step — and interact much more strongly with bound $Pt(NO_2)_4^{2-}$ ions (Fig. 13B), increasing the destabilizing effect of Cl^- on $Pt(NO_2)_4^{2-}$ binding and also increasing the degree of coupling that occurs between the movement of the two ionic species inside the pore. In effect, in the R334Q/I344K double pore mutant, one kind of antagonistic Cl^-:blocker interaction (Fig. 13A) has been replaced by another with a different molecular mechanism (Fig. 13B). Presumably in I344K channels both knock-off mechanisms shown in Fig. 13A, B are in effect.

4.4. Understanding the observed properties of $Pt(NO_2)_4^{2-}$ block of I344K channels

Block of I344K/E1371Q by cytoplasmic $Pt(NO_2)_4^{2-}$ was previously described as being of very high affinity, very strong voltage dependence, and very high sensitivity to extracellular $[Cl^-]$ [47]. The model shown in Fig. 13B can provide an explanation for each of these properties. This mutant shows elevated $Pt(NO_2)_4^{2-}$ binding affinity (Fig. 8D, E; Table 2) because, as described above, there is an additional positive charge to interact electrostatically with the blocking anion. Elevated voltage dependence of block results not from increased intrinsic voltage-dependence of $Pt(NO_2)_4^{2-}$ binding itself (Fig. 8D; Table 2), but from increased voltage-dependence of external Cl^- binding (Fig. 8F; Table 2) and more strongly voltage-dependent $Pt(NO_2)_4^{2-}$ binding to Cl^--occupied channels (Fig. 8E; Table 2) that is proposed to reflect strongly coupled movement of $Pt(NO_2)_4^{2-}$ and Cl^- ions inside the pore. These explanations suggest that it is altered channel interactions with Cl^-, rather than with $Pt(NO_2)_4^{2-}$ itself, that are responsible for the observed increase in the voltage-dependence of $Pt(NO_2)_4^{2-}$ block. Increased sensitivity to extracellular $[Cl^-]$ results both from an increase in Cl^- binding affinity (Fig. 8F; Table 2), perhaps reflecting the creation of a novel Cl^- binding site inside the pore (Fig. 13B), and also from an increased sensitivity of bound $Pt(NO_2)_4^{2-}$ ions to the binding of Cl^- (Fig. 9C). In this model, block is more Cl^--sensitive because the mutant inner vestibule can accommodate both $Pt(NO_2)_4^{2-}$ and Cl^- ions that bind in a strongly antagonistic fashion (Fig. 13B).

4.5. Relevance to the mechanism of Cl^- conduction

In many ion channel types, antagonistic ion–ion interactions are thought to be required to couple tight ion binding with the rapid ion throughput associated with channel-mediated transport (see Introduction). Such a mechanism has been proposed previously for CFTR [33,34] and is illustrated in Fig. 13C. Physiological relevance of interactions between Cl^- ions bound in the inner vestibule and outer vestibule is supported by the finding that mutations that neutralize the positive charge at either K95 [49,50,63] or R334 [33] (Fig. 13C) are associated with a dramatic decrease in unitary Cl^- conductance. Reduced conductance in K95Q is restored in K95Q/I344K, leading to the proposal that a positive charge located at either of these two nearby residues is able to support physiologically important Cl^- binding in the inner vestibule [35, 50]. However, although I344K appears capable of restoring sensitivity to external Cl^- ions that is lost in R334Q, this does not result in a significant restoration of unitary Cl^- conductance (Fig. 12). In other words, although it is suggested that in R334Q/I344K channels one form of knock-off inside the pore has been replaced by another (Fig. 13B), this surrogate knock-off mechanism does not appear to be capable of supporting high Cl^- conductance in the way that normal ion–ion interactions in wild type CFTR are proposed to do (Fig. 13C, D). This suggests that it is not enough simply to have multiple Cl^- ions bound inside the pore concurrently that can interact with one another to generate rapid Cl^- flux. Presumably the locations of the anion binding sites in the inner and outer vestibules (Fig. 1) — and the ability of anions bound concurrently to these two sites to interact with one another — are crucial for the normal, rapid Cl^- permeation mechanism. One possibility is that the interaction between anions bound to the two sites illustrated in Fig. 13C is not directly electrostatic as has been proposed in Ca^{2+} [14] and K^+ channels [18], but instead that mutually antagonistic anion binding to the outer and inner vestibule binding sites occurs at a distance, perhaps *via* a rapid conformational change in the protein that alters anion binding affinity. The present study therefore supports a multi-ion mechanism of Cl^- permeation in CFTR, although perhaps not a classical electrostatic knock-on mechanism.

Transparency document

The Transparency document associated with this article can be found, in the online version.

Acknowledgements

I would like to thank Christina Irving and Dr. Yassine El Hiani for their assistance with this work supported by the Canadian Institutes of Health Research and Cystic Fibrosis Canada.

References

[1] E. Gouaux, R. MacKinnon, Principles of selective ion transport in channels and pumps, Science 310 (2005) 1461–1465.
[2] D.A. Doyle, J.M. Cabral, R.A. Pfuetzner, A. Kuo, J.M. Gulbis, S.L. Cohen, B.T. Chait, R. MacKinnon, The structure of the potassium channel: molecular basis of K^+ conduction and selectivity, Science 280 (1998) 69–77.
[3] Y. Zhou, J.H. Morais-Cabral, A. Kaufman, R. MacKinnon, Chemistry of ion coordination and hydration revealed by a K^+ channel–Fab complex at 2.0 Å resolution, Nature 414 (2001) 43–48.
[4] J. Payandeh, T. Scheuer, N. Zheng, W.A. Catterall, The crystal structure of a voltage-gated sodium channel, Nature 475 (2011) 353–358.
[5] X. Zhang, W. Ren, P. DeCaen, C. Yan, X. Tao, L. Tang, J. Wang, K. Hasegawa, T. Kumasaka, J. He, J. Wang, D.E. Clapham, N. Yan, Crystal structure of an orthologue of the NaChBac voltage-gated sodium channel, Nature 486 (2012) 130–134.
[6] L. Tang, T.M. Gamal El-Din, J. Payandeh, G.Q. Martinez, T.M. Heard, T. Scheuer, N. Zheng, W.A. Catterall, Structural basis for Ca^{2+} selectivity of a voltage-gated calcium channel, Nature 505 (2014) 56–61.
[7] R. Dutzler, E.B. Campbell, M. Cadene, B. Chait, R. MacKinnon, X-ray structure of ClC chloride channel at 3.0 Å reveals the molecular basis of anion selectivity, Nature 415 (2002) 287–294.
[8] R. Dutzler, E.B. Campbell, R. MacKinnon, Gating the selectivity filter in ClC chloride channels, Science 300 (2003) 108–112.
[9] S. Lobet, R. Dutzler, Ion-binding properties of the ClC chloride selectivity filter, EMBO J. 25 (2006) 24–33.
[10] H. Jayaram, A. Accardi, F. Wu, C. Williams, C. Miller, Ion permeation through a Cl^- selective channel designed from a CLC Cl^-/H^+ exchanger, Proc. Natl. Acad. Sci. U. S. A. 105 (2008) 11194–11199.
[11] R.E. Hibbs, E. Gouaux, Principles of activation and permeation in an anion-selective Cys-loop receptor, Nature 474 (2011) 54–60.
[12] V.K. Dickson, L. Pedi, S.B. Long, Structure and insights into the function of a Ca^{2+}-activated Cl^- channel, Nature 516 (2014) 213–218.
[13] B. Hille, Ion Channels of Excitable Membranes, 3rd edn Sinauer Associates, Sunderland, 2001.
[14] W.A. Sather, E.W. McCleskey, Permeation and selectivity in calcium channels, Annu. Rev. Physiol. 65 (2003) 133–159.
[15] B. Roux, Ion conduction and selectivity in K^+ channels, Annu. Rev. Biophys. Biomol. Struct. 34 (2005) 153–171.
[16] R. Horn, B. Roux, J. Åqvist, Permeation redux: thermodynamics and kinetics of ion movement through potassium channels, Biophys. J. 106 (2014) 1859–1863.
[17] C.M. Armstrong, Life among the axons, Annu. Rev. Physiol. 69 (2007) 1–18.
[18] D.A. Köpfer, C. Song, T. Gruene, G.M. Sheldrick, U. Zachariae, B.L. de Groot, Ion permeation in K^+ channels occurs by direct Coulomb knock-on, Science 346 (2014) 352–355.

[19] A.L. Hodgkin, R.D. Keynes, The potassium permeability of a giant nerve fibre, J. Physiol. 128 (1955) 61–88.
[20] B. Hille, W. Schwartz, Potassium channels as multi-ion single-file pores, J. Gen. Physiol. 72 (1978) 409–442.
[21] J. Neyton, C. Miller, Discrete Ba^{2+} block as a probe of ion occupancy and pore structure in the high-conductance Ca^{2+}-activated K^+ channel, J. Gen. Physiol. 92 (1988) 569–586.
[22] J. Bormann, O.P. Hamill, B. Sakmann, Mechanism of anion permeation through channels gated by glycine and γ-aminobutyric acid in mouse cultured spinal neurones, J. Physiol. 385 (1987) 243–286.
[23] D.R. Halm, R.A. Frizzell, Anion permeation in an apical membrane chloride channel of a secretory epithelial cell, J. Gen. Physiol. 99 (1992) 339–366.
[24] G.Y. Rychkov, M. Pusch, M.L. Roberts, T.J. Jentsch, A.H. Bretag, Permeation and block of the skeletal muscle chloride channel, ClC-1, by foreign anions, J. Gen. Physiol. 111 (1998) 653–665.
[25] Z. Qu, H.C. Hartzell, Anion permeation in Ca^{2+}-activated Cl^- channels, J. Gen. Physiol. 116 (2000) 825–844.
[26] J.P. Reyes, A. López-Rodriguez, A.E. Espino-Saldaña, A. Huanosta-Gutiérrez, R. Miledi, A. Martinez-Torres, Anion permeation in calcium-activated chloride channels formed by TMEM16A from *Xenopus tropicalis*, Pflugers Arch. 466 (2014) 1769–1777.
[27] J.A. Tabcharani, J.M. Rommens, Y.-X. Hou, X.-B. Chang, L.-C. Tsui, J.R. Riordan, J.W. Hanrahan, Multi-ion pore behaviour in the CFTR chloride channel, Nature 366 (1993) 79–82.
[28] P. Linsdell, J.A. Tabcharani, J.W. Hanrahan, Multi-ion mechanism for ion permeation and block in the cystic fibrosis transmembrane conductance regulator chloride channel, J. Gen. Physiol. 110 (1997) 365–377.
[29] Z. Zhou, S. Hu, T.-C. Hwang, Probing an open CFTR pore with organic anion blockers, J. Gen. Physiol. 120 (2002) 647–662.
[30] X. Gong, P. Linsdell, Coupled movement of permeant and blocking ions in the CFTR chloride channel pore, J. Physiol. 549 (2003) 375–385.
[31] X. Gong, P. Linsdell, Mutation-induced blocker permeability and multiion block of the CFTR chloride channel pore, J. Gen. Physiol. 122 (2003) 673–687.
[32] B. Lubamba, B. Dhooghe, S. Noel, T. Leal, Cystic fibrosis: insight into CFTR pathophysiology and pharmacotherapy, Clin. Biochem. 45 (2012) 1132–11144.
[33] X. Gong, P. Linsdell, Maximization of the rate of chloride conduction in the CFTR chloride channel pore by ion–ion interactions, Arch. Biochem. Biophys. 426 (2004) 78–82.
[34] P. Linsdell, Mechanism of chloride permeation in the cystic fibrosis transmembrane conductance regulator chloride channel, Exp. Physiol. 91 (2006) 123–129.
[35] P. Linsdell, Cystic fibrosis transmembrane conductance regulator chloride channel blockers: pharmacological, biophysical and physiological relevance, World J. Biol. Chem. 26 (2014) 26–39.
[36] S. McDonough, N. Davidson, H.A. Lester, N.A. McCarty, Novel pore-lining residues in CFTR that govern permeation and open-channel block, Neuron 13 (1994) 623–634.
[37] D.N. Sheppard, K.A. Robinson, Mechanism of glibenclamide inhibition of cystic fibrosis transmembrane conductance regulator Cl^- channels expressed in a murine cell line, J. Physiol. 503 (1997) 333–346.
[38] P. Linsdell, J.W. Hanrahan, Substrates of multidrug resistance-associated proteins block the cystic fibrosis transmembrane conductance regulator chloride channel, Br. J. Pharmacol. 126 (1999) 1471–1477.
[39] X. Gong, S.M. Burbridge, A.C. Lewis, P.Y.D. Wong, P. Linsdell, Mechanism of lonidamine inhibition of the CFTR chloride channel, Br. J. Pharmacol. 137 (2002) 928–936.
[40] M.-S. Li, A.F.A. Demsey, J. Qi, P. Linsdell, Cysteine-independent inhibition of the CFTR chloride channel by the cysteine-reactive reagent sodium (2-sulphonatoethyl) methanethiosulphonate (MTSES), Br. J. Pharmacol. 157 (2009) 1065–1071.
[41] M.-S. Li, R.G. Holstead, W. Wang, P. Linsdell, Regulation of CFTR chloride channel macroscopic conductance by extracellular bicarbonate, Am. J. Physiol. 300 (2011) C65–C74.
[42] R. MacKinnon, C. Miller, Mechanism of charybdotoxin block of the high-conductance, Ca^{2+}-activated K^+ channel, J. Gen. Physiol. 91 (1988) 335–349.
[43] X. Gong, P. Linsdell, Molecular determinants and role of an anion binding site in the external mouth of the CFTR chloride channel pore, J. Physiol. 549 (2003) 387–397.
[44] N. Ge, P. Linsdell, Interactions between impermeant blocking ions in the CFTR chloride channel pore. Evidence for anion-induced conformational changes, J. Membr. Biol. 210 (2006) 31–42.
[45] J.-J. Zhou, P. Linsdell, Evidence that extracellular anions interact with a site outside the CFTR chloride channel pore to modify channel properties, Can. J. Physiol. Pharmacol. 87 (2009) 387–395.
[46] M.-S. Li, E.A. Cowley, P. Linsdell, Pseudohalide anions reveal a novel extracellular site for potentiators to increase CFTR function, Br. J. Pharmacol. 167 (2012) 1062–1075.
[47] P. Linsdell, State-dependent blocker interactions with the CFTR chloride channel: implications for gating the pore, Pflugers Arch. 466 (2014) 2243–2255.
[48] J.-J. Zhou, M. Fatehi, P. Linsdell, Direct and indirect effects of mutations at the outer mouth of the cystic fibrosis transmembrane conductance regulator chloride channel pore, J. Membr. Biol. 216 (2007) 129–142.
[49] J.-J. Zhou, M.-S. Li, J. Qi, P. Linsdell, Regulation of conductance by the number of fixed positive charges in the intracellular vestibule of the CFTR chloride channel pore, J. Gen. Physiol. 135 (2010) 229–245.
[50] Y. El Hiani, P. Linsdell, Tuning of CFTR chloride channel function by location of positive charges within the pore, Biophys. J. 103 (2012) 1719–1726.
[51] H.N. Rubaiy, P. Linsdell, Location of a permeant anion binding site in the cystic fibrosis transmembrane conductance regulator chloride channel pore, J. Physiol. Sci. (2015)http://dx.doi.org/10.1007/s12576-015-0359-6.
[52] P. Linsdell, Functional architecture of the CFTR chloride channel, Mol. Membr. Biol. 31 (2014) 1–16.
[53] S.D. Broadbent, M. Ramjeesingh, C.E. Bear, B.E. Argent, P. Linsdell, M.A. Gray, The cystic fibrosis transmembrane conductance regulator is an extracellular chloride sensor, Pflugers Arch. (2015)http://dx.doi.org/10.1007/s00424-014-1618-8.
[54] M. Spassova, Z. Lu, Coupled ion movement underlies rectification in an inward-rectifier K^+ channel, J. Gen. Physiol. 112 (1998) 211–221.
[55] J.A. Tabcharani, P. Linsdell, J.W. Hanrahan, Halide permeation in wild-type and mutant cystic fibrosis transmembrane conductance regulator chloride channels, J. Gen. Physiol. 110 (1997) 341–354.
[56] P. Linsdell, Thiocyanate as a probe of the cystic fibrosis transmembrane conductance regulator chloride channel pore, Can. J. Physiol. Pharmacol. 79 (2001) 573–579.
[57] P. Linsdell, J.W. Hanrahan, Adenosine triphosphate-dependent asymmetry of anion permeation in the cystic fibrosis transmembrane conductance regulator chloride channel, J. Gen. Physiol. 111 (1998) 601–614.
[58] D. Oliver, H. Hahn, C. Antz, J.P. Ruppersberg, B. Fakler, Interaction of permeant and blocking ions in cloned inward-rectifier K^+ channels, Biophys. J. 74 (1998) 2318–2326.
[59] J. Thompson, T. Begenisich, Interaction between quaternary ammonium ions in the pore of potassium channels. Evidence against an electrostatic repulsion mechanism, J. Gen. Physiol. 115 (2000) 769–782.
[60] Q. Ma, E. Pavlov, T. Britvina, G.W. Zamponi, R.J. French, Trans-channel interactions in batrachotoxin-modified rat skeletal muscle sodium channels: kinetic analysis of mutual inhibition between μ-conotoxin GIIIA derivatives and amine blockers, Biophys. J. 95 (2008) 4266–4276.
[61] L. Yang, J. Edvinsson, L.G. Palmer, Interactions of external K^+ and internal blockers in a weak inward-rectifier K^+ channel, J. Gen. Physiol. 140 (2012) 529–540.
[62] M. Spassova, Z. Lu, Tuning the voltage dependence of tetraethylammonium block with permeant ions in an inward rectifier K^+ channel, J. Gen. Physiol. 114 (1999) 415–426.
[63] N. Ge, C.N. Muise, X. Gong, P. Linsdell, Direct comparison of the functional roles played by different membrane spanning regions in the cystic fibrosis transmembrane conductance regulator chloride channel pore, J. Biol. Chem. 279 (2004) 55283–55289.
[64] J.-P. Mornon, B. Hofmann, S. Jonic, P. Lehn, I. Callebaut, Full-open and closed CFTR channels, with lateral tunnels from the cytoplasm and an alternative position of the F508 region, as revealed by molecular dynamics, Cell. Mol. Life Sci. 72 (2015) 1377–1403.